The Contribution of Oscillatory Activity to the Modulation of Different Sensorimotor Circuits

Under Varying Working Memory Load

by

Nicholas Eric Barclay

A thesis

presented to the University of Waterloo

in fulfillment of the

thesis requirement for the degree of

Master of Science

in

Kinesiology

Waterloo, Ontario, Canada, 2022

AUTHOR'S DECLARATION

I hereby declare that I am the sole author of this thesis. This is a true copy of the thesis, including any required final revisions, as accepted by my examiners. I understand that my thesis may be made electronically available to the public.

ABSTRACT

Goal-directed movement requires a series of highly coordinated voluntary motor outputs, which need to adequately integrate information from the body's internal and external environments to be executed successfully. The integration of sensory information to inform motor output is known as sensorimotor integration. Sensorimotor integration involves afferent projections to the primary motor cortex (M1) via multiple sensorimotor loops. These sensorimotor loops eventually converge on the corticospinal neuron (CSN) to determine motor out. However, the specific groups or circuits of interneurons targeted by the different sensorimotor loops are not known. The current study combined controllable pulse parameter transcranial magnetic stimulation (cTMS) with electroencephalography (EEG) to assess the association between oscillatory brain activity in different brain regions and sensorimotor integration in the M1 measured by short-latency afferent inhibition (SAI). To facilitate the quantification of any association, both oscillatory brain activity and SAI were measured during a working memory task under varying working memory demands. SAI circuits were probed using three different cTMS configurations, posterior-anterior (PA) current with a 120 μs duration (PA120), anterior-posterior (AP) current with a 120 μs duration (AP120) and AP current with a 30 μs duration (AP30). Increased working memory load reduced SAI across all three current configurations. However, the magnitude of the reduction decreased from PA120 to AP120 to AP30. SAI-EEG associations revealed that the effect of working memory load on SAI was modulated by the amount of parietal alpha and frontocentral low beta activity. The current results suggest several sensorimotor circuits converge on the CSN, all receiving similar projections from various brain regions under working memory load. It seems that distinctions across the circuits are dependent on other unique modulatory projections, which are not probed by working memory load.

ACKNOWLEDGEMENTS

TABLE OF CONTENTS

LIST OF FIGURES

LIST OF ABBREVIATIONS

AP – Anterior - Posterior

APB – Abductor Pollicis Brevis

CSN – Corticospinal Neuron

cTMS - Controllable pulse parameter Transcranial Magnetic Stimulation

D – Direct

EEG - Electroencephalography

EMG – Electromyography

ERS – Event-Related Synchronization

ERSP - Event-Related Spectral Perturbation

FDI - First Dorsal Interosseous

GABAA – Gamma-Aminobutyric Acid A

GABAB - Gamma-Aminobutyric Acid

BHREB - Human Research Ethics Board

I – Indirect

ISI – Interstimulus Interval

M1 – Primary Motor Cortex

MEP – Motor-Evoked Potential

N - Negative

P - Positive

PA - Posterior-Anterior

PTN – Pyramidal Tract Neuron

S1 – Sensory Cortex

SAI - Short-latency Afferent Inhibition

SEP – Somatosensory Evoked Potential

SMA – Supplementary Motor Area

SMU – Sensory Motor Unit

TMS - Transcranial Magnetic Stimulation

1.0 INTRODUCTION

For skilled action involving complex motor patterns and accurate motor learning to take place, integration of sensory information from the body's internal and external environment (known as sensorimotor integration) is necessary. The primary motor cortex (M1), responsible for the eventual motor output, receives input from various sensorimotor loops converging on its corticospinal neurons (CSN). The various inputs to the CSNs contribute to shaping the resulting movement. These sensorimotor loops represent a diverse array of neural networks. Consequently, their impact on the motor output varies depending on the type of movement being performed and a large variety of other factors. These factors include but are not limited to influences such as motor learning, perception, motivation, context, brain state, and disease. For instance, primary somatosensory sensorimotor loops may inhibit afferent projections to reduce task-irrelevant muscle contractions during skilled behaviours (Pfurtscheller et al., 1996; Pfurtscheller & Lopes da Silva, 1999). Frontoparietal sensorimotor loops may be more goal-oriented and incorporate a top-down approach through cognitive control processes, such as attention (Stefan et al., 2004). In contrast, posterior parietal sensorimotor loops may reflect crossmodal interactions between the senses (Edwards et al., 2019). While these sensorimotor loops' existence and general function are known, the nuances of how these loops interact in M1 to shape sensorimotor output are not well understood.

Sensorimotor integration can be examined in several ways to determine the origin and function of the various sensorimotor projections to the motor cortex. One particular method is through a technique known as transcranial magnetic stimulation (TMS), a non-invasive form of brain stimulation. TMS uses magnetic fields to induce current flow in the brain, which, when strong enough, produces an action potential, mimicking the natural communication process in the

brain (Trachina & Nicholson, 1986). When TMS is delivered over the M1 , the induced

excitation of the cortical spinal neurons leads to an evoked response in the corresponding muscle

known as a motor-evoked potential (MEP). If TMS is combined with a preceding peripheral

stimulus, the output of the CSNs is inhibited leading to a reduced MEP, a phenomenon known as

short-latency afferent inhibition (SAI). The extent of the inhibition is tied to the strength of the

afferent information relayed to motor cortex (Bailey et al., 2016). Therefore, SAI is a valuable

tool in studying the contribution of different sensorimotor loops converging in the motor cortex.

Not only is SAI sensitive to the strength of the afferent projection, but SAI is also sensitive to

cognitive constructs, such as attention and working memory (Mirdamadi et al., 2017; Suzuki &

Meehan, 2018). Therefore, SAI may reflect combinations of sensorimotor circuits acting on the

CSN. The recent emergence of controllable pulse parameter TMS (cTMS) has enhanced our

ability to better define, specific groups or circuits of interneurons. Therefore, by changing the

direction or duration of the TMS stimulus over the M1 it may be possible to disentangle the

targets of various sensorimotor loops converging on the CSN (Hannah & Rothwell, 2017;

Mirdamadi et al., 2017; Suzuki & Meehan, 2018).

Another common method used to infer the activity of superficial brain regions and networks

is electroencephalography (EEG). EEG measures intracranial electrical currents through

corresponding voltages on the scalp (Loo & Barkley, 2005). Observing the rhythmic fluctuations

in voltage, or "oscillatory activity", is one way to link specific brain functions or processes to

particular brain regions (Loo & Barkley, 2005). This ability to non-invasively measure brain

activity is especially powerful when combined with other modalities such as SAI. Associating

oscillatory activity from different brain regions with SAI in the motor cortex can provide insight

into the origin of afferent input to the specific sensorimotor circuit recruited by the cTMS

stimulus. Such associations will provide a greater understanding of the significance of these sensorimotor circuits to sensorimotor integration and behaviour.

1.1 Sensorimotor Circuits

It is well understood that the process of sensorimotor integration is an integral part of motor control and learning. Sensorimotor integration allows for the dynamic integration of sensory information from the environment to inform an intentional motor response (Machado et al., 2010). However, details regarding the process itself are still not well understood. Determining the specific contribution of each brain region, their synergies, and respective sensorimotor loops is a difficult task. The task is further complicated by the specific contributions of different brain areas being dynamic and influenced by a multitude of factors, including current brain state (Crochet et al., 2019). The primary goal of this study is to enhance our understanding of the afferent input to the various sensorimotor circuits that converge on the motor cortex CSN by assessing oscillatory activity at the time SAI is assessed.

Two basic principles dictate how brain regions, and by extension, their sensorimotor loops, are organized regarding sensorimotor integration. The first is that any region responsible for movement production has some form of somatotopic representation of the body (Machado et al., 2010). This is believed to be a crucial component relating to how such precise movement patterns are generated so consistently and accurately (Machado et al., 2010).

The second principle is a hierarchical order of the brain regions involved in sensorimotor control. The hierarchy consists of three levels, the most inferior being the medullar, followed by the subcortical and then cortical regions (Machado et al., 2010). The medullar level is responsible for associating afferent information from the skin, muscles, and joints. It is

responsible for basic movement patterns consisting of stereotyped motor outputs, like the withdrawal reflex (Machado et al., 2010). These medullary outputs are often too simplistic for most tasks and are often overridden by more complex descending projections from the superior levels (Machado et al., 2010). The subcortical level is responsible for selecting and organizing spinal motor programs involved in postural stabilization. The subcortical level also plays a primary role in making anticipatory postural adjustments to voluntary movement (Machado et al., 2010). The final layer is within the cerebral cortex, which consists of association areas that are neither entirely motor nor sensory. These association areas integrate many forms of sensory information and their activity is shaped by various cognitive aspects such as attention, emotion, planning, and memory (Machado et al., 2010).

Several functional elements are consistent across all sensorimotor loops. Understanding what is consistent across all sensorimotor loops is an important first step in identifying the critical differences in individual sensorimotor loops. First, spinal synergies are likely a fundamental component of motor control. The recruitment pattern of these synergies is dictated mainly by brain regions that relay cortical output to the corticospinal tract (Bizzi & Ajemian, 2020). This comes from the theory that diverse motor behaviors are the result of the combination of spinal muscle groupings or "synergies", each with different timing and scaling factors (Bizzi et al. 2000). These synergies are believed to simplify the control of movement by making it so broader motor commands can be given out, as opposed to controlling individual muscles (Bizzi & Ajemian, 2020).

Another common factor across all sensorimotor loops is they all incorporate at least one of the cortical output regions regardless of whether they are located in the spinal cord, midbrain, or cortex (Bizzi & Ajemian, 2020). Furthermore, while each sensorimotor loop serves a unique

functional role, there is also some redundancy (Bizzi & Ajemian, 2020). The redundancy in the

sensorimotor system, combined with the fact that it is distributed across multiple brain regions,

highlights the need for developing a complete understanding of the individual sensorimotor loops

(Bizzi & Ajemian, 2020). Without an understanding of the individual circuits, it makes it very

difficult to determine the actual contributions of each region and network involved. The

continuous converging of these loops also feeds back on itself and results in not only

manipulating motor output but also loop activity in itself, which adds yet another layer of

complexity (Bizzi & Ajemian, 2020).

Out of all of the sensorimotor loops, the cortical loops are what should be focused on, as

they are responsible for the most complex and relevant movements. They are also the highest on

the sensorimotor control hierarchy, meaning that their outputs override those at the lower levels

(Machado et al., 2010). The following paragraphs briefly outline each of the major cortical

loops.

The fronto-parietal loop consists of direct anatomical connections between the premotor

cortex, parietal cortex, and the dorsal premotor area (Pandya et al., 1969). This loop is

multifunctional and is believed to integrate afferent input from multiple modalities, such as gaze

direction and limb proprioception, to accurately judge reaching tasks (Wise & Kurata, 1989). It

is also believed to be responsible for the selection of alternative actions (Pesaran et al., 2008), in

addition to hand grasping movements (Lehmann & Scherberger, 2013).

At least three known cortico-thalamic loops connect the motor cortex with the thalamus

(Bizzi & Ajemian, 2020). Previous work has found that before all movement, there is a period of

preparatory activity (Lara et al., 2018). In some cases, the preparatory period before movement

results in a delay (Economo et al., 2018). The three known cortico-thalamic loops all appear to

have the same general function of maintaining the activity of M1 neurons during the delayed

period of movement preparation (Bizzi & Ajemian, 2020). Several cells from layer 5 of the M1

have reciprocal projections with thalamic nuclei (Bizzi & Ajemian, 2020). Premotor cortex also

has reciprocal projections with the thalamic nuclei (Bizzi & Ajemian, 2020). The third loop is

between the thalamus and cerebellum, which will be discussed in more detail regarding cortico-

cerebellar loops (Bizzi & Ajemian, 2020).

While there are multiple projections from the basal ganglia involved in many cognitive-

motor functions, there is a primary "motor circuit," which receives projections from M1, primary

somatosensory areas, parietal area Brodmann Area 5 and premotor areas spanning Brodmann

Area 6; as well as the supplementary motor area (SMA) (Bizzi & Ajemian, 2020). This motor

circuit is believed to organize and segment motor actions into chunks (Bizzi & Ajemian, 2020).

As mentioned previously, this greatly eases the amount of processing that needs to be done by in

this case, the putamen, allowing for groupings of submovements to be processed, as opposed to a

series of individual submovements (Bizzi & Ajemian, 2020).

Regarding cortico-cerebellar loops, previous work has shown there is an anatomical closed-

loop circuit between M1 and specific regions of the cerebellar cortex (Kelly & Strick, 2003).

Specifically, Purkinje cells in lobules 4 and 6 of the cerebellar cortex, have reciprocal projections

with the region of the M1 responsible for controlling the arm (Kelly & Strick, 2003). The

reciprocal nature of these projections demonstrates the closed loop nature of cortico-cerebellar

interactions (Kelly & Strick, 2003). The cortico-cerebellar loop being a closed loop is an

important distinction as it means that it does not need to rely on outside input for feedback (Kelly

& Strick, 2003). Furthermore, it is believed that the cortico-cerebellar loop plays a crucial part in

the temporal component of the recruitment of spinal synergies (Berger et al., 2020). This is

counter to other motor cortical areas which are believed to be involved with determining the

spatial structure of the spinal synergies (Berger et al., 2020).

Having looked at some of the major sensorimotor loops, it is clear that the primary cortical

output regions for most sensorimotor loops are the primary motor or premotor cortices, while a

lesser portion output through other areas such as the SMA, cingulate motor area, and a portion of

area 5 (Rathelot & Strick, 2009). It is also apparent that the resulting corticospinal outputs from

the major sensorimotor loops consist of signals from a diverse range of brain regions that

converge on pyramidal neurons in M1 to shape motor output (Rathelot & Strick, 2009). There

currently is no global theory of sensorimotor loop coordination, resulting in most investigators

simply identifying what each respective brain region is "encoding" (Bizzi & Ajemian, 2020).

However, this only tells part of the story. Due to the complex interactions involved in

sensorimotor control, simply correlating movement variables to neural activity is not enough.

When the redundancy across several sensorimotor loops is taken into account, it becomes

difficult to determine which signals correlate to the resulting motor output and which are

artifacts. Hence, taking a more representational approach, only using indirect measures such as

EEG, is ineffective. Instead, observing specific sensorimotor loops through stimulation of

specific circuits is the ideal way to tease apart these various connections. One of the ways to do

this non-invasively is using a brain stimulation method like TMS.

1.2 Transcranial Magnetic Stimulation (TMS)

Non-invasive brain stimulation provides an effective method to determine the impact of a

particular brain state or behaviour on motor cortex output. It can aid in the identification of

particular circuits and sensorimotor loops. One such non-invasive brain stimulation method is

TMS. TMS uses an electromagnetic field to induce current flow in the brain. If the induced

7

current crosses with an axon and is strong enough to elicit suprathreshold polarization, it produces an action potential (Trachina & Nicholson, 1986).

TMS applied over the M1 elicits a series of high-frequency descending corticospinal volleys or "waves" that result in an evoked muscle twitch called a MEPs response (Day et al., 1989). When the volley is due to direct activation of corticospinal axons, it is referred to as a direct (D) wave (Rothwell et al., 1991). As the D-wave results from directly exciting the corticospinal axon, it is the shortest latency volley recorded. However, the elicitation of a D-wave is not a common phenomenon (Hallett, 2007). Directly exciting the CSN requires extremely high intensities with an induced current in an atypical lateral-medial direction (Rothwell et al., 1991). The high intensities are often outside the TMS device's capability or untenable for the participant. As such, this approach is rarely employed. Instead, a current is typically induced at lower intensities using either posterior-anterior (PA) or, less commonly, the anterior-posterior (AP) directions. The descending volleys elicited by PA or AP current occur at increasingly longer latencies than the D-wave at intervals of approximately 1.5 ms (Hallett, 2007). As a result, the volleys' timing induced by PA and AP current reflects the synaptic inputs of interneurons to the CSN and are referred to as indirect (I) waves. I-waves are numbered according to their relative position (I1, I2, I3…) and are often categorized as early (I1, I2) or late (I3, I4...) (Rothwell et al., 1991).

As noted, current can be induced in either a PA or AP direction using TMS. The majority of research conducted up to this point using TMS has employed PA-induced current, despite that there are differences in I-wave recruitment between the two directions. Both directions illicit I1, I2 and I3 waves. However, PA-directed current primarily recruits early I-waves but can recruit late I-waves at higher intensities, whereas AP current primarily recruits late I-waves (I3, I4) (Day

et al. 1989; Di Lazzaro et al., 2001). This difference was first thought to reflect a subpopulation of cortical neurons activated by AP stimulation that are activated by PA stimulation. However, the presence of multiple I-waves raises questions about their functional significance.

It appears that the interneurons recruited by PA and AP stimuli have distinct anatomical inputs and pathways. This is seen in a study using cerebellar TMS to assess cerebellar-M1 connectivity (Spampinato et al., 2020). The study found that the time point after cerebellar stimulation that had the maximum effect on M1 varied between PA and AP (Spampinato et al., 2020). Specifically, a timing difference of 2-3 ms longer for MEPs evoked by AP stimulation as opposed to PA was found (Spampinato et al., 2020). The extra time needed for AP stimulation is likely due to it taking a different and slightly longer sensorimotor circuit from the cerebellum to the M1. This is in line with a recent model that depicts AP currents inputs to the M1 being further from the pyramidal neuron, whereas PA stimulation has a direct input (Aberra et al., 2020). TMS is an extremely useful tool for directly studying motor circuits, although, on its own, it is difficult to study how motor circuits interact with sensory afference. To better understand how these unique circuits relate to functions like sensorimotor integration, one can use a TMS technique that incorporates sensory afference, called SAI.

1.3 Short-latency Afferent Inhibition (SAI)

Afferent inhibition is the reduction in the TMS evoked MEP when the TMS stimulus is preceded by electrical stimulation of the corresponding sensory nerve. In the case of SAI, the interstimulus interval (ISI) for maximum inhibition to occur is ~20 ms for median nerve stimulation and ~25ms for digit stimulation (Bikmullina et al., 2009; Ni et al., 2011). The inhibition occurs in the cortex as the afferent signal from the digit or wrist is timed to converge on the CSNs of M1 at TMS onset (Tokimura et al., 2000). These converging signals cause reduced excitability in the

M1, resulting in the reduced amplitude of the I2 and I3 waves elicited by TMS (Tokimura et al., 2000). The magnitude of SAI is directly related to the strength of the sensory afferent volley induced by the peripheral conditioning stimulus (Bailey et al., 2016). The amount of inhibition will increase until all of the nerve's afferent fibers are recruited (Bailey et al., 2016). SAI is also somatotopically organized in the hand, meaning that homotopic stimulation (afferent stimulation near the target muscle), produces greater inhibition than heterotopic stimulation (afferent stimulation distant from the target muscle) (Dubbioso et al., 2017). This also coincides with the general principle of sensorimotor integration, that all regions involved in motor control are somatotopically organized. Somatosensory evoked potentials (SEPs) produced by the same peripheral stimulus indicate sensory cortex (S1) activity is associated with SAI and potentially induced by S1 projections to the M1 (Bailey et al., 2016). S1 has long-range horizontal monosynaptic excitatory projections that can influence the upper layers of M1 and are believed to excite GABAergic inhibitory cells inducing SAI (Bailey et al., 2016).

Several pharmacological studies have provided insight into the neurophysiology behind SAI. Studies which administered lorazepam to participants, a Gamma-Aminobutyric Acid A-receptor (GABAA) agonist, show reduced SAI supporting the theory that SAI is partially mediated by GABAergic circuits (Turco et al., 2018a). Although it appears to be the case for specifically GABAA, when using baclofen, a GABA B-receptor (GABAB) agonist, it does not appear to alter SAI (Turco et al., 2018a). SAI also seems to be mediated by cholinergic circuits (Di Lazzaro et al., 2000). SAI is significantly decreased by the acetylcholine antagonist scopolamine (Di Lazzaro et al., 2000). The cholinergic influence on SAI is also supported by alterations in patients with neurodegenerative disorders of the central cholinergic system, including Alzheimer's disease (Di Lazzaro et al., 2005) and Parkinson's disease (Celebi et al.,

2012). The mechanisms behind this are unclear. It could simply be reducing sensory input to the motor cortex and therefore reducing inhibition, or it could have a direct effect on inhibitory areas of the motor cortex (Di Lazzaro et al., 2000).

In addition to pharmacological/physiological influences, SAI is modulated by the state of the target muscle, the task-relevance of the muscle and cognitive factors. For instance, there is reduced SAI immediately before and during the movement of the target muscle (Asmussen et al., 2013). The cause of the SAI reduction is believed to be due to the gating of somatosensory afference, as the reduction in SAI during the pre-movement phase does not alter spinal excitability, as F-waves, which correspond with spinal activation, remain unchanged (Asmussen et al., 2013). Conversely, there is elevated SAI in M1 muscle representations not associated with an ongoing motor behaviour (Asmussen et al., 2014). An elevation in SAI in uninvolved motor areas suggests that SAI is modulated based on the muscle's intended action and the muscle's relevance to the action (Turco et al., 2018b). Changes in working memory and attention demand also appear to influence SAI (Simon et al., 2016; Mirdamadi et al., 2017; Suzuki & Meehan, 2018). The influence of working memory and attentional demands on SAI demonstrates that SAI can be used to quantify the various synaptic pathways that modulate how attentional mechanisms influence motor output.

Multiple factors such as working memory and attention influencing the differences between PA and AP stimulus are consistent with the idea that TMS output, along with motor output in general, depends on multiple sensorimotor inputs and not a single circuit. It also appears that the activity levels related to these particular networks have a specific impact depending on the circuit involved. This is seen in the excitability for the AP current direction

being more dependent on cerebellar activity than for the PA direction (Hamada et al., 2014; Spampinato et al., 2020).

Recently there has been the development of a new form of TMS, called cTMS, which allows for control of stimulus pulse duration. The relatively new ability to manipulate pulse duration reveals that specific pulse durations preferentially recruit unique sets of neural circuits. It appears that a shorter pulse duration of 30 μs for AP current (AP30) produces longer latency MEPs compared to a longer pulse duration of 120 μs for AP currents (AP120) (D'Ostilio et al., 2016; Hannah & Rothwell, 2017). Traditional TMS pulses are ~82 μs in duration (Rothkegel et al., 2010). In particular, Hannah and Rothwell (2017) demonstrated that AP30 currents produced peaks of the sensory motor unit firing for several milliseconds longer than those evoked by PA120. It was also found that the AP120 stimulus evoked a combination of the durations seen for AP30 and PA120. The same study showed that the PA120 and AP120 currents were more sensitive to voluntary contraction than AP30. These both suggest that AP30 recruits a different set of inputs than AP120. Although, it should also be noted that there were minimal differences between AP currents regarding SAI at rest (Hannah & Rothwell, 2017). The lack of difference at rest is believed to be because during a resting state, the threshold is increased, therefore requiring a greater stimulus intensity which is more likely to activate a variety of CSN inputs (Hannah & Rothwell, 2017). There were also no differences seen in SAI across the PA current direction, implying that PA stimulus is consistent regardless of current duration (Hannah & Rothwell, 2017).

The previously mentioned changes in excitability brought on by cerebellar activity also appear to be specific to current duration and not just direction. Specifically, it appears that

cerebellar activity modulates the AP30 current duration but not for AP120, demonstrating yet

another distinction of the AP30 stimulus duration (Hannah & Rothwell, 2017).

A recent modelling study further supports the existence of unique circuits/networks

related to each stimulus type and proposes the potential regions within M1 where I waves are

generated (Aberra et al., 2020). The PA circuit is suggested to preferentially activate the synaptic

terminals of layer 5 (L5) pyramidal neurons within M1, close to the central sulcus (Aberra et al.,

2020). Conversely, the AP circuit preferentially activates the layers 2 and 3 (L2/3) pyramidal

neurons within M1 (Aberra et al., 2020). It was also suggested that PA stimulation would

directly activate corticomotoneuronal cells monosynaptically within L5, producing shorter

latency MEPs (Aberra et al., 2020). Whereas AP stimulation is indirect and likely activates

rostral M1 or pre-motor pyramidal cells producing MEPs polysynaptically with longer latencies

(Aberra et al., 2020). The proposed differences in latency align with the findings that PA

stimulus preferentially produces earlier I waves, compared to AP (Di Lazzaro et al., 2001). The

implication of direct stimulation for PA circuits also would explain why motor thresholds are

generally lower for PA stimulation. Using SAI on its own, however, would not allow this

model's validity to be proven. SAI only allows for conclusions to be drawn about the individual

sensorimotor circuit being stimulated from the resulting motor output. SAI does not inform us

about the several indirect inputs converging on the sensorimotor circuit. Getting a better

understanding of those indirect inputs, would require the introduction of an additional measure

like EEG, which allows for indirect measures of brain activity, for the entire brain at a given

time.

1.4 Electroencephalography (EEG)

EEG allows for indirect measures of brain activity from a variety of cortical regions within the brain. EEG functions by measuring intracranial electrical currents through corresponding voltages on the scalp (Loo & Barkley, 2005). When neurons in the brain are activated, it produces flows of electrical current localized to the region where the activation occurred (Teplan, 2002). Specifically, EEG measures the currents generated by the post-synaptic potentials of pyramidal neurons in the cerebral cortex (Teplan, 2002). The majority of measurable EEG signals come from the cerebral cortex. Yet, these signals are generally weak as they are attenuated by the thickness of the skull and other layers between the cluster of neurons firing and the electrode recording the signal on the scalp (Teplan, 2002). These impediments are also the reason why the signal from the scalp electrode must be massively amplified before being recorded (Teplan, 2002) and why signals from deeper cortex and subcortical structures are extensively attenuated and difficult to assess using surface electrodes.

There are two primary ways of analyzing EEG data. The first is through studying evoked potentials (EP) or event-related potentials (ERPs). The second is through quantifying the relative contributions of voltage fluctuations in various frequencies that make up the time-locked EEG signal (Lansbergen et al., 2011). The contributions of the various frequencies is measured via the power spectral perturbations compared to a specific baseline.

EPs represent consistent activity related to an external stimulus, while ERPs are related to endogenous processes (Beres, 2017). EPs and ERPs are extracted by time-locking and averaging epochs to a particular event to enhance the signal to noise of the neural activity tied to that particular event (Thompson et al., 2008). In particular, ERPs are extremely useful tools for

investigating various aspects of cognitive processes, such as language comprehension and production, visual processing, memory, and attention, amongst many others (Beres, 2017).

SEPs are a set of brain events tied to the processing of a somatosensory stimulus and sensorimotor integration. SEPs are recorded over the somatosensory areas of the brain and represent specifically the processing of mechanical, thermal, or chemical sensory stimuli. As a general rule of thumb, it is believed that earlier components represent basic, low-level perception and are automatic, occurring whenever there is a change or a new stimulus presented (Beres, 2017). Conversely, later components, typically after 250 ms, represent conscious cognitive processing, which can be elicited by various experimental conditions (Beres, 2017).

The significance of each peak is task-dependent, and several early SEPs appear to be critical to somatosensory processing and sensorimotor integration as a whole. Positive waves are represented with a P, and negative waves are followed with an N, both of which are then followed by a number, which often represents the time from the start of the ERP that the peak occurred (Beres, 2017). One of these SEPs is the N20, which is the earliest occurring cortical response to mechanical cutaneous stimulation (Mauguiere, 2005). In support of this earliest arrival of somatosensory afference, the N20 has been localized to area 3b of S1 (Allison et al., 1991). The N20 has been shown to respond to contralateral tactile stimuli, implying the N20 has a role in sensorimotor integration (Dancey et al., 2016). The role of the N20 in sensorimotor integration is also seen when N20 amplitude increases during motor learning. N20 amplitude increasing during motor learning also demonstrates the importance of the S1 in motor learning and sensorimotor integration (Dancey et al., 2016).

Another key SEP is the frontal N30. The frontal N30 is generated in the precentral gyrus's premotor and supplementary motor areas. The frontal N30 is linked to the cortico-thalamic

15

sensorimotor loop consisting: of the thalamus, premotor areas, basal ganglia, and M1 (Cebolla et al., 2011). The frontal N30's role in the cortico-thalamic sensorimotor loop is the activation of the circuit at M1 concerning sensorimotor integration (Cebolla et al., 2011). The N30 has also been shown to increase following motor learning acquisition (Dancey et al., 2016).

The second way of studying EEG data is through the analysis of the rhythmic fluctuation of voltage, commonly called "oscillatory activity" (Lansbergen et al., 2011). Under this model of EEG analysis, five primary frequency bins are studied: delta (0–3.5 Hz), theta (3.5–8 Hz), alpha (8–12 Hz), beta (13–30 Hz), and gamma (30–70 Hz) (De Pascalis et al., 2020). The relative contribution of a specific frequency band to the overall EEG signal has been linked to a range of cognitive processes, emotional states, and behaviour (De Pascalis et al., 2020). Similar to EPs and ERPs, the EEG signal is locked to a specific stimulus or event and the changes in the contributions of the different frequency bands is expressed as a ratio or percentage of a baseline period to produce an event-related spectral perturbation (ERSP) measure (Li et al., 2021). The change in the ERSP measure for a specific frequency can be used to infer changes in task-related processes and correlated to performance metrics.

Delta oscillations are primarily associated with cognitive processing (Başar et al., 1999). Delta wave activity has been linked to signal matching and decision-making processes and appears to decrease following increases in cognitive and motor requirements (Karakaş et al., 2000). Based on the findings that delta activity decreases with increased workload, it is believed that the delta frequency represents degrees of consciousness (Karakaş et al., 2000). This is further supported by the fact that increased levels of delta wave activity are seen during slow-wave sleep, which is believed to be the deepest form of sleep, and when rapid eye movement sleep occurs (Knyazev, 2012).

Theta oscillations are associated with both motor and cognitive processes (Shin, 2011). Theta activity has been closely correlated with voluntary motor activity during tasks such as walking, running, rearing, jumping, swimming, digging, and manipulating objects (Shin, 2011). Specifically, greater theta activity is seen during movement initiation and execution compared to periods of rest or stillness (Cruikshank et al., 2012). The motor findings regarding theta activity are likely closely linked to the cognitive findings. Theta activity correlates with selective attention, which would be required to accurately direct movement (Başar et al., 2001). Theta activity has also been shown to modulate arousal levels, with excessive or highly increased amounts of theta activity being linked to reduced arousal levels (Lazzaro et al., 1999). It is through this manipulation of arousal, that theta oscillations are believed to direct attention (Başar et al., 2001). This is seen in theta activities associated with orienteering, a coordinated process that indicates levels of alertness and arousal, or in other words, a subject's readiness to process information (Başar et al., 2001). Along with directing attention, theta activity is also associated with other cognitive processes, like memory encoding (Dushanova & Christov, 2014). Specifically, theta modulation is theorized to be responsible for memory-related interactions involving the prefrontal cortex and medial temporal lobe (Anderson et al., 2010).

Alpha oscillations are associated with both motor and cognitive processes (Dushanova & Christov, 2014). With regards to motor control, alpha has been associated with cortical idling, as alpha activity in the motor cortex has been shown to decrease upon movement onset (Pfurtscheller et al., 1997). Alpha synchronization has also been seen in the motor cortex during non-motor visual encoding tasks such as reading (Pfurtscheller et al., 1996). Alpha band activity is also believed to be demonstrative of working memory and attentional processes (Jensen et al., 2002). Similar to changes in theta frequency, this demonstrates the closely related nature of

attention directing working memory. Greater alpha activity has been seen in older subjects

compared to younger subjects during sensory processing, further showing the link between alpha

and sensorimotor integration (Dushanova & Christov, 2014). This increase is believed to be

caused by differences in attention levels across the groups (Dushanova & Christov, 2014).

Regarding the specific sensorimotor loops involved, alpha is primarily generated by cortico-

cortical and thalamo-cortical neuronal networks (Da Silva et al., 1980).

Beta oscillations are associated with both motor and cognitive processes (Schmidt et al.,

2019). A commonly seen phenomenon found in nearly every subject after finger, hand, arm, and

foot movement is post-movement beta event-related synchronization (ERS). Post-movement

beta ERS has been shown to have a somatotopic organization and at maximum levels results in

reduced excitability of motor cortex neurons (Pfurtscheller & Lopes da Silva, 1999).

Furthermore, beta desynchronization is often seen over sensorimotor areas during voluntary

movement and is believed to be responsible for helping maintain muscle contraction (Engel &

Fries, 2010). Beta frequencies have also been linked to executive movement control, with

increased frontal beta synchronization being related to successful stop trials during a stop-signal

task (Schmidt et al., 2019). Increases in frontal beta also are believed to inhibit working memory.

Increased frontal beta aids in the elimination of distractions during movement, which prevents

the encoding of memories by eliminating the necessary cues and information by deeming them

as distractions (Schmidt et al., 2019). Furthermore, just as frontal beta is believed to cancel an

ongoing motor response, it is also believed to cancel long-term memory retrieval (Schmidt et al.,

2019).

Gamma oscillations are associated with both motor and cognitive processes (Minc et al.,

2010). Regarding motor control, during dynamic force output, it is believed that the sensorimotor

system switches to relaying information via higher frequencies (Omlor et al., 2007). Gamma is

believed to be the primary higher frequency used. Using a higher frequency allows for faster

integration of visual and somatosensory information, which is required for the proper motor

response to be made in time (Omlor et al., 2007). This is demonstrated by the subsequent

decrease in the beta frequency during a dynamic motor response, compared to relatively no

change in the gamma frequency (Omlor et al., 2007). That being said, gamma oscillations do not

necessarily appear to be related to any one particular motor or cognitive process, but instead are

responsible for the binding of related cortical elements involved in almost all major processes,

including attention, memory, motor planning, sensorimotor integration and cognition (Minc et

al., 2010).

Overall, EEG provides a useful resource for understanding how task-related changes in

brain activity at various brain regions result in changes in both motor output and cognition. Of

the two primary methods of EEG analysis, ERPs often provide a more nuanced measure.

However, they cannot always be collected due to timing differences. Both methods provide

evidence to support the concept of multiple sensorimotor loops being simultaneously involved in

sensorimotor integration. This background on SAI and EEG measures gives way to my original

conceptual model of EEG frequency's impact on SAI, which was developed before conducting

the study.

1.5 Conceptual Model

My starting conceptual model proposed a direct link between the amount of SAI produced during

a verbal working memory task and changes in EEG frequency related to SEP amplitude,

specifically, the N20-P25 and P20-N30 SEPs. This was based on work by Mirdamadi et al.

(2017), who found that an increased demand on attentional resources during a visual detection

task led to reduced AP SAI but had no effect on PA SAI. This coincided with findings that the frontal P20-N30 SEP also reduced with increased attentional demands, while the parietal N20-P25 SEP did not change (Mirdamadi et al. 2017). Therefore, it was suggested that the frontal P20-N30 SEP was linked with AP SAI, while the parietal N20-P25 SEP was linked with PA SAI (Mirdamadi et al. 2017). The link between the N20-P25 SEP and PA SAI was also supported by other previous work (Bailey et al., 2016). When developing the model, it was acknowledged that the findings of Suzuki and Meehan (2018) were contradictory: increased working memory demands reduced SAI for both PA and AP stimulation, accompanied by a reduction in parietal N20-P25 SEP. However, this would contradict the theory that there were separate I-wave generators for AP stimulation, so it was deemed less likely since the theory of separate I-wave generators has substantial support from previous work (Day et al. 1989; Di Lazzaro et al., 2001).

The results of the Mirdamadi et al. (2017) paper were then combined with the findings of a distinct difference in SAI production, with AP30 producing greater amounts of SAI, compared to AP120, PA120, and PA30, which all produced relatively similar results (Hannah & Rothwell, 2017). Since no distinction was seen regarding stimulus duration across the PA stimulus, it was believed that PA stimulation recruited the same circuit regardless of stimulus duration. The Mirdamadi et al. (2017) results were then used to explain the difference seen in AP30, theorizing that AP30 current was influenced primarily by the frontal P20-N30 generator, whereas AP120 and both PA currents were influenced by the parietal N20-P25 generator, seen in Figure 1.

Assuming that the SAI differences were due to differences in SEP influence, that would then mean that each current configuration generator could be identified using EEG. Therefore, it was theorized that PA120 and AP120 stimulation could be associated with the parietal N20-P25 generator through an event-related desynchronization parietal alpha frequency, as was seen in
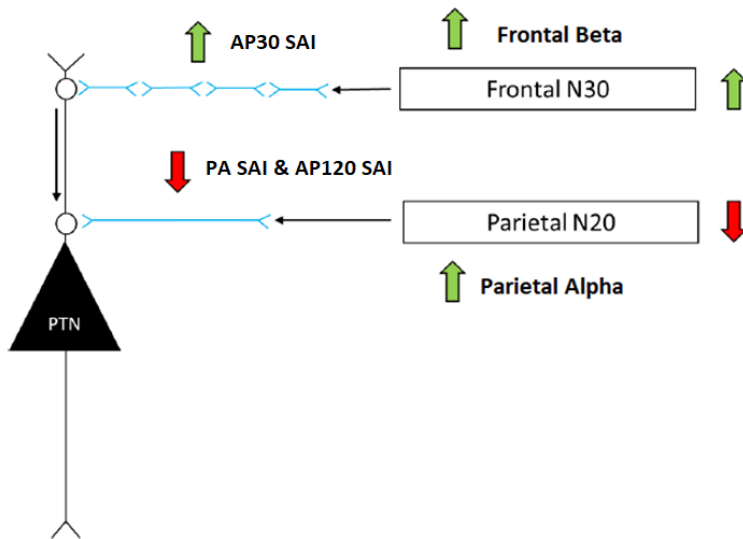
Figure 1- My original conceptual model. It depicts the pathways of the sensorimotor signal for each TMS current direction into the pyramidal tract neuron (PTN). The blue lines indicate neurons. The green arrows indicate an increase in amount. The red arrows indicate a decrease in amount.

visual encoding tasks (Pfurtscheller et al., 1996), whereas AP30 stimulation could be associated

with the frontal P20-N30 generator through an ERS in frontal beta frequency. This was chosen

due to the frontal ERS being associated with the elimination of irrelevant stimuli, and stopping

tasks, which was linked to the SMA, a potential origin for the frontal P20-N30 generator

(Schmidt et al., 2019; Stančák Jr et al., 2000). This proposed relationship is also seen in Figure 1.

2.0 AIMS AND HYPOTHESES

The two major aims and associated hypotheses were developed under the assumption that there would be differences in the magnitude of SAI produced by TMS due to both current direction and duration.

Aim #1: To elaborate on previous work done in this lab and establish the difference in SAI between AP30, AP120 and PA120 during a verbal working memory task.

Hypothesis #1: It was hypothesized under a higher verbal working memory load, there would be decreased SAI in AP120 and PA120, but an increase in AP30.

Aim #2: Establish a relationship between SAI of MEPs elicited by TMS and frequency of EEG signal, differentiating between the various types of TMS stimulus (PA120, AP120, AP30) .

Hypothesis #2A: It was hypothesized that increases in parietal alpha ERS would be associated with increased working memory demand a reduction in PA120 SAI and AP120 SAI.

Hypothesis #2B: Conversely, it was proposed that increased frontal beta ERS would relate to increased working memory demand and AP30 SAI.

3.0 METHODS

3.1 Participants

Eighteen adults (18 right-handed, 4 male, 14 female, 24 ± 2 years old) with no history of neurological disease or contraindications to TMS provided informed consent and participated in the experiment. The results of four participants were dropped from the analysis due to being unable to generate adequate MEPs during the AP30 current stimulation. An additional participant was dropped from the analyses due to scoring less than 60%, at all but the lowest difficulty level. Therefore, whether they were actually engaging working memory or simply guessing could not be determined. The study protocol was approved by the University of Waterloo Human Research Ethics Board (HREB).

3.2 Experimental Design and Procedure

The experiment consisted of a single session. Participants performed 300 trials of a modified Sternberg working memory task. To manipulate the working memory load, set size (2, 4, 6, 8 or 10 letters) varied across trials.

EEG was recorded throughout the task. Simultaneously, SAI was assessed during the specific period of the working memory task where participants actively maintained a set of letters in working memory. To determine the influence of working memory load on different sensorimotor circuits, SAI was assessed using three different transcranial magnetic stimuli. For 100 trials, the TMS stimulus used to assess SAI consisted of a 30 µs width stimulus that induces an anterior-posterior current in the underlying tissue (AP30). Another 100 trials induced an anterior-posterior current with a pulse width of 120 µs (AP120). The remaining 100 trials induced a PA current with a pulse width of 120 µs (PA120). The direction of the current was a

result of passing a current through the TMS coil windings in the PA direction for AP or the

anterior-posterior direction for PA. Further, the ISI between the peripheral conditioning stimulus

and the TMS stimulus used to assess SAI was 21 ms. The trial order was consistent for each

block of 100 trials, consisting of a combination of unconditioned and conditioned trials, with

each set containing one of each difficulty level. However, the blocks were presented in a

pseudorandomized order, which varied between participants.

In total, participants completed 10 trials for each combination of TMS stimuli, SAI ISI

and memory set size (Figure 2).

3.3 Behavioural Task

The verbal working memory task was a variant of the Sternberg short-term memory task.

Participants were seated in front of a computer screen with their left index and middle finger

positioned on a keyboard at adjacent response keys. A trial started with the presentation of a

central fixation cross for 400 msec (Figure 3). After 400 ms, a set of 2, 4, 6, 8 or 10 letters

appeared at various locations around the fixation cross. Participants were instructed to memorize

this set of letters (Encoding phase). After 2500 ms, the set of letters disappeared (Maintenance

phase). After 3000 ms, a probe replaced the fixation cross, and participants were required to

respond whether the probe was, or was not, part of the initial memory set. For 50% of the trials,

the probe was drawn from the initial memory set. The probe was drawn from a letter that was not

in the initial memory set for the remaining trials. The probe was displayed for 1500 ms, after

which the next trial began. The "Yes" and "No" response keys were randomized across

participants. The response time and accuracy of each trial was recorded. Response time was

derived from all correct responses. Incorrect responses consisted of trials in which the participant

pressed the wrong key or failed to respond while the probe was displayed on the screen.

PA120 (100 Trials)									
Control (50 Trials)					SAI 21 (50 Trials)				
2 Letters	4 Letters	6 Letters	8 Letters	10 Letters	2 Letters	4 Letters	6 Letters	8 Letters	10 Letters
10 Trials	10 Trials	10 Trials	10 Trials	10 Trials	10 Trials	10 Trials	10 Trials	10 Trials	10 Trials

↓

AP120 (100 Trials)									
Control (50 Trials)					SAI 21 (50 Trials)				
2 Letters	4 Letters	6 Letters	8 Letters	10 Letters	2 Letters	4 Letters	6 Letters	8 Letters	10 Letters
10 Trials	10 Trials	10 Trials	10 Trials	10 Trials	10 Trials	10 Trials	10 Trials	10 Trials	10 Trials

↓

AP30 (100 Trials)									
Control (50 Trials)					SAI 21 (50 Trials)				
2 Letters	4 Letters	6 Letters	8 Letters	10 Letters	2 Letters	4 Letters	6 Letters	8 Letters	10 Letters
10 Trials	10 Trials	10 Trials	10 Trials	10 Trials	10 Trials	10 Trials	10 Trials	10 Trials	10 Trials

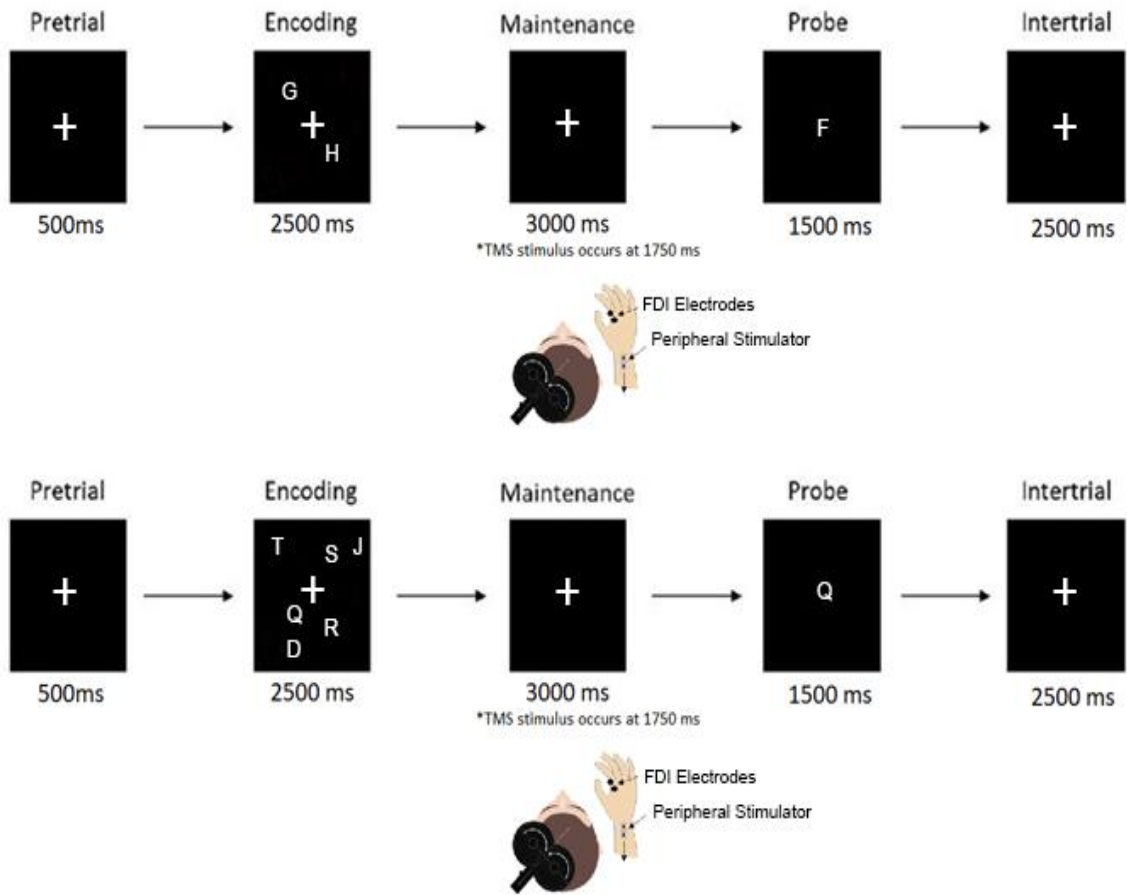*Figure 2- The breakdown of trials within each 100 trial block for each stimulus width.*

Figure 3- Outline of the verbal working memory task for 2 and 6-letter trials.

3.4 Electroencephalography (EEG)

Electroencephalographic data was recorded from 30 electrode sites using sintered Ag/AgCl TMS compatible electrodes (EasyCap, Brain Vision Solutions). Electrodes were placed in accordance with the 10-20 international system and referenced to the right mastoid. All channel recordings had an impedance of < 5kΩ. EEG data were filtered (DC-200 Hz, 6dB octave roll-off) and digitized (1000 Hz, SynAmps 2, Neuroscan) before being stored for offline analysis.

ERSPs were extracted using the EEGLab toolbox (Institute for Neural Computation, University of California – San Diego, San Diego, CA) for MATLAB v2020b (The MathWorks, Natick, MA) environment. Prior to derivation of the ERSP, the continuous EEG files were time-locked to the onset of the encoding phase, with the pretrial phase acting as the baseline. The resulting epochs started 500 ms prior to the presentation of the memory set (encoding phase) and ended 23 ms prior to the onset of the TMS stimulus to ensure that no noise from the TMS stimulus interfered with the signal. The data was filtered using a bandpass filter (2–50 Hz, 6dB rolloff). Each epoch was then visually analysed and any epoch that featured excessive noise was removed. An independent components analysis was then run to identify EEG signal relating to eye movements and blinks. Any independent component(s) related to ocular artifacts were removed from the overall EEG signal. ERSPs were then extracted from the epoched data, using a wavelet filter (3 cycles, 0.5 min/max) and 200-time points (20 ms per time point). The resulting spectral results were by average baseline to express the ERSP as a proportion of the baseline. The ERSP were derived for five different frequency bands by average the ERPS values across the specific frequency range from 2500 ms to 4227 ms after the letters appeared at the FCz and CP3 electrode sites. The frequency ranges used for each frequency bin were: theta (6-8 Hz), alpha (8-12 Hz), low beta (13-18 Hz), high beta (18-30 Hz) and gamma (30-45 Hz). See Figure

4. CP3 and FCz were chosen as these are the electrodes where the parietal N20-P25 and frontal N30 SEPs, previously linked to PA and AP SAI, are maximal.

3.5 Transcranial Magnetic Stimulation (TMS)

Motor evoked potentials elicited by TMS were recorded using custom LabVIEW 2016 software (National Instruments, Austin, Tx) coupled with an AC amplifier (HP-511, Astro Med Grass, Oakville, ON) and analog-to-digital board (NI-USB 6341, National Instruments, Austin, TX). Surface electromyography (EMG) electrodes (Ag-AgCl) were placed on the right first dorsal interosseous (FDI) and abductor pollicis brevis (APB) muscles using a tendon belly montage. The EMG recording was triggered using a 5 V TTL pulse with an epoch of 0.3 to 0.5 s. During acquisition, data was amplified (x1000), digitized (x40,000 Hz) and filtered (bandpass filtered 5–1000 Hz, notch filter – 60 Hz). Surface EMG was then down-sampled to 5000 Hz during offline analysis. An MEP was defined as the peak-to-peak amplitude of the maximal electromyographic response between 20 and 50 ms post-TMS stimulation.

The TMS was delivered using a controllable pulse parameter TMS stimulator (cTMS; Rogue Research, Montreal, Québec, Canada) to elicit MEPs during the maintenance phase. Participants were seated with their arms bent and supported on a desk in front of them. The TMS coil was oriented tangentially to the scalp with the handle positioned 45° posterior to the midline. The same positioning was used for both PA and anterior-posterior (AP) stimulation. The current direction was specified using custom coils.
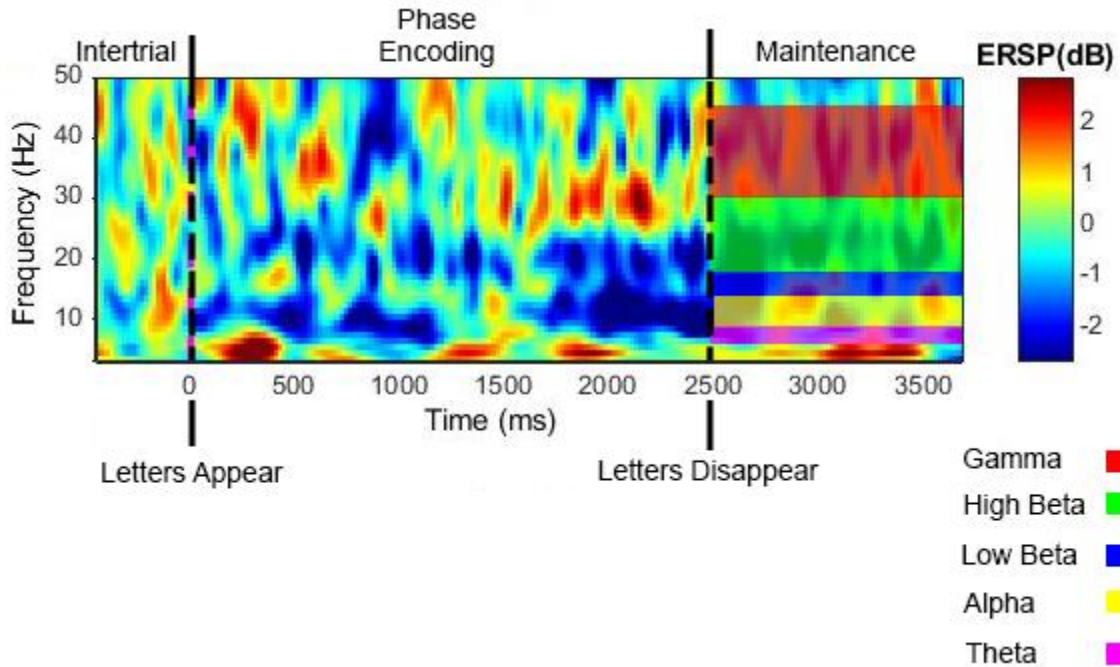
Figure 4 - A representative spectrogram from an individual subject.. The first dashed line indicates the end of the Intertrial phase and the beginning of the Encoding Phase. The second dashed line indicates the beginning of the Maintenance phase. Each coloured band in the Maintenance phase represents the respective frequency band which is being studied.

The left FDI motor cortical hotspot was defined as the scalp position, which elicited the largest MEP in the FDI most consistently following Posterior Anterior (PA) stimulation. The same hotspot was used for AP stimulation. The coil's positioning at the hotspot was recorded using the BrainSight™ stereotactic system (Rogue Research, Montreal, Québec, Canada). The stimulus intensity needed to elicit an MEP of 1 mV was determined using a sequential tracking (ML-PEST) adaptive threshold-hunting method (Awiszus, 2003). The ML-PEST method used a binary, yes or no response to model an S-shaped function of the probabilistic nature of evoking a motor potential. The ML-PEST method was conducted by adjusting stimulus intensity via the instructions provided from the TMS Motor Threshold Assessment Tool (MTAT 2.0) software (Clinical Research Solutions, Charleston, South Carolina). The 1 mV stimulus intensity procedure was repeated for both the PA and AP induced currents, absent of peripheral stimulation.

3.6 Short-Latency Afferent Inhibition (SAI)

A DS7A constant current high voltage stimulator (Digitimer North America LLC, Fort Lauderdale, Florida, USA) was placed over the right median nerve. The peripheral electrical stimulus was then set to an intensity which produced a slight thumb twitch (Abbruzzese et al., 2001). The stimulus was applied in a constant current square wave pulse with 0.2 ms duration, cathode proximal (Mirdamadi et al., 2017). The electrical stimulus intensity was set to 2.6 ± 0.9 times sensory threshold, which was defined as the intensity which participants correctly identified the presence/absence of stimulation on five out of 10 trials (Suzuki & Meehan, 2018). This was the intensity that was used during the experiment task. For the unconditioned trials, there was no peripheral electrical stimulus, and during the SAI trials it preceded TMS

stimulation by 21 ms (SAI₂₁). An ISI of 21ms is known to produce the greatest inhibition for PA (Tokimura et al., 2000; Ni et al., 2011) and AP SAI (Ni et al., 2011).

MEPs recorded during the SAI₂₁ trials were compared with MEPs elicited during the unconditioned trials. The amount of SAI produced was reported as a percentage of the unconditioned MEP (**Error! Reference source not found.**5).

3.7 Data Analysis

Statistical analyses were conducted using the R environment for statistical computing (R Development Core Team, 2019).

The average ERSP amplitudes and MEP values were first calculated across all participants for all TMS configurations (AP30, AP120, PA120), separated by working memory load (Low, High) and electrode (FCz, CP3). Low load was determined for each subject as the first difficulty level where their accuracy was less than 95%. High load was determined for each subject as the first difficulty level where their accuracy was at or less than 70%. To read the processed ERSP and EMG data into R the "readxl" package was used.

Hypothesis #1 was first addressed by confirming SAI was sensitive to verbal working memory load. This was done by running a linear mixed model with the fixed factors of Load (Low, High) and TMS configuration (AP30, AP120, PA120). Subject was included as a random factor. The linear mixed models were run using the "lme4" package and the model output was gotten using the "lmerTest" package. Main effects and interactions were decomposed using post-tests to compare the estimated marginal means. Estimated marginal means were run using the

$$\% \text{ SAI } = \frac{\text{Condioned } MEP}{Unconditioned\ MEP} \ x\ 100$$

Figure 5- Calculation for percentage of SAI

"emmeans" package. Bonferroni correction was used to address family-wise error rates, where applicable. The Bonferroni corrections were run using the "rstatix" package. The η_p^2 and cohens f effect size measures were also run using the "sjstats" package. The average latencies between the onset of TMS stimulus and the resulting MEP were also calculated.

Hypotheses #2A and #2B were then addressed, determining if frequency had a meaningful effect on SAI. This was done by including Load, TMS Configuration and Frequency as fixed effects in a linear mixed model. Load and TMS Configuration were categorical fixed effects. ERSP amplitude was included as a continuous fixed effect. Subject was again included as a random factor. Separate linear mixed models were run for each frequency bin (Theta, Alpha, Low Beta, High Beta, Gamma) and electrode site (CP3, FCz). The main effects of Load or TMS Configuration were decomposed by comparing the estimated marginal means. Any effect involving ERSP amplitude was decomposed by comparing the estimated marginal trends (e.g. slopes). The packages "jtools" and "interactions" were used to plot the interactions between the ratio of the unconditioned MEP and ERSP amplitude.

4.0 RESULTS

4.1 Participants

Eighteen adults (18 right-handed, 4 male, 14 female, 24 ± 2 years old) with no history of neurological disease or contraindications to TMS provided informed consent and participated in the experiment. The results of three participants were dropped from the analysis due to being unable to generate adequate MEPs during the AP30 current stimulation. An additional participant was dropped from the analyses due to scoring less than 60%, at all but the lowest difficulty level. Therefore, it could not be determined whether they were actually engaging working memory or simply guessing.

4.2 Behaviour

ANOVAs were run to test the effect of load on the accuracy and reaction time data. The purpose of these tests was to ensure that no speed-accuracy trade-off was present in the data. A two-way repeated measures ANOVA for task accuracy revealed a significant main effect of Load $\left[F_{1,55} = 74.96, \ p = 7.481\mathrm{e}^{-12}, \eta_p^2 = 0.17\right]$. Neither the main effect of TMS Type $\left[F_{2,55} = 1.55, \ p = 0.22, \eta_p^2 = 0.08\right]$ or the TMS Type by Load interaction $\left[F_{2,55} = 0.32, \ p = 0.73, \eta_p^2 = 0.02\right]$ were significant. The main effect of Load was driven by a significant decrease in accuracy as Load increased from Low to High [Low: 92±2%, mean±standard error, High: 72±2%] See **Error! Reference source not found.**.

The two-way repeated measures ANOVA for reaction time revealed a significant main effect of Load $\left[F_{1,55} = 14.88, \ p = 0.0003, \eta_p^2 = 0.21\right]$ and TMS Type $\left[F_{2,55} = 4.91, \ p = 0.01, \eta_p^2 = 0.15\right]$. However, the TMS Type by Load interaction $\left[F_{2,55} = 0.32, \ p = 0.72, \eta_p^2 = 0.01\right]$ was not significant. The main effect of Load was driven by a significant decrease in
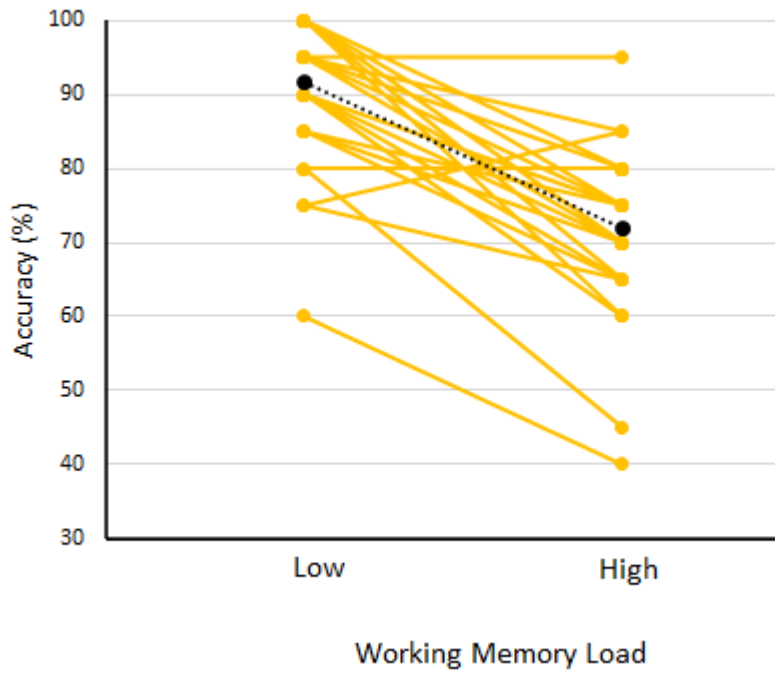
Figure 6- Accuracy (%) vs. Working Memory Load. Accuracy represents the amount of incorrect working memory trials divided by the amount of incorrect working memory trials.

accuracy as Load increased from Low to High [Low: 0.76±0.02 ms, mean±standard error, High: 0.83±0.02%] The main effect of TMS Type was driven by a significantly lower reaction time for AP30, compared to PA120 and AP120 [PA120: 0.81±0.02 ms, mean±standard error, AP120: 0.81±0.02 ms, AP30: 0.74±0.02 ms] See **Error! Reference source not found.**7.

4.3 Short-Latency Afferent Inhibition (SAI):

MEP latency was calculated. The MEP latency for PA120 was 21.0 ms, AP120 latency was 22.3 ms and AP30 latency was 22.9 ms. See Figure 8.

A linear mixed model was run to determine if SAI is sensitive to load by comparing Load (Low, High) by TMS Type (PA120, AP120, AP30), with subject as a random factor. There was a significant main effect of Load $\left[F_{1,60} = 12.02, \ p = \ 0.00098, \ \eta_p^2 = 0.17\right]$, and a strong trend for a significant main effect of TMS type $\left[F_{2,60} = \ 2.74, \ p = \ 0.073, \ \eta_p^2 = 0.08; \ PA120 = \right.$ $\left. 0.71 \pm \ 0.062, AP120 = \ 0.58 \pm \ 0.062, AP30 = \ 0.64 \pm \ 0.062\right]$. There was no significant effect for the two-way interaction of Load x TMS Type $\left[F_{1,60} = 0.51, p = 0.60, \ \eta_p^2 = 0.02\right]$. The significant main effect of load was a result of a 15.7% decrease in SAI from Low Load [0.564%±0.0575] (mean ± standard error) to High Load [0.769%±0.721], regardless of TMS Type. See Figure 99. The average latencies for each stimulus type were also calculated. There was an average difference of 1.3 ms between PA120 and AP120 stimulus and a difference of 1.9 ms between PA120 and AP30 stimulus. See Figure 8.
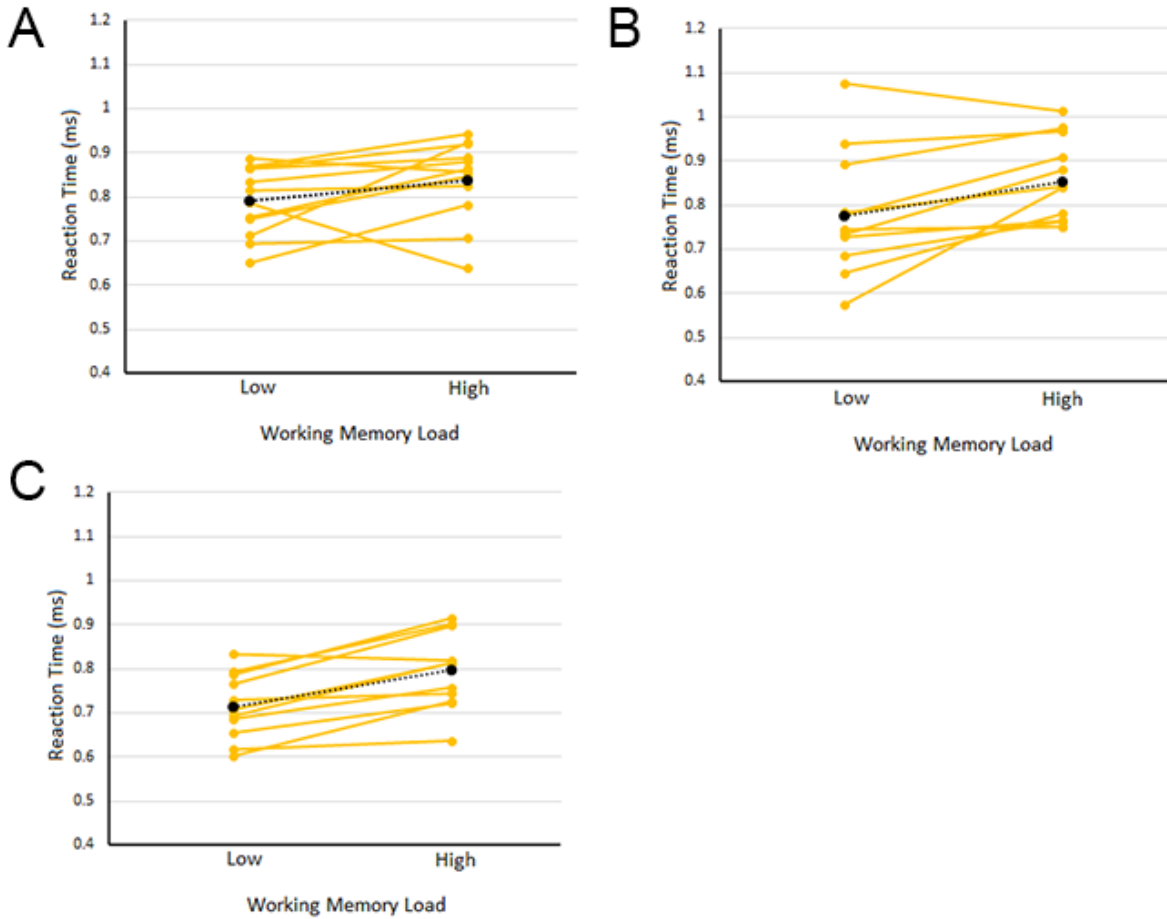
Figure 7- Reaction Time (ms) vs Working Memory Load for A: PA120, B: AP120 and C: AP30. Reaction time represents the average amount of time it took for a participant to respond to the probe.
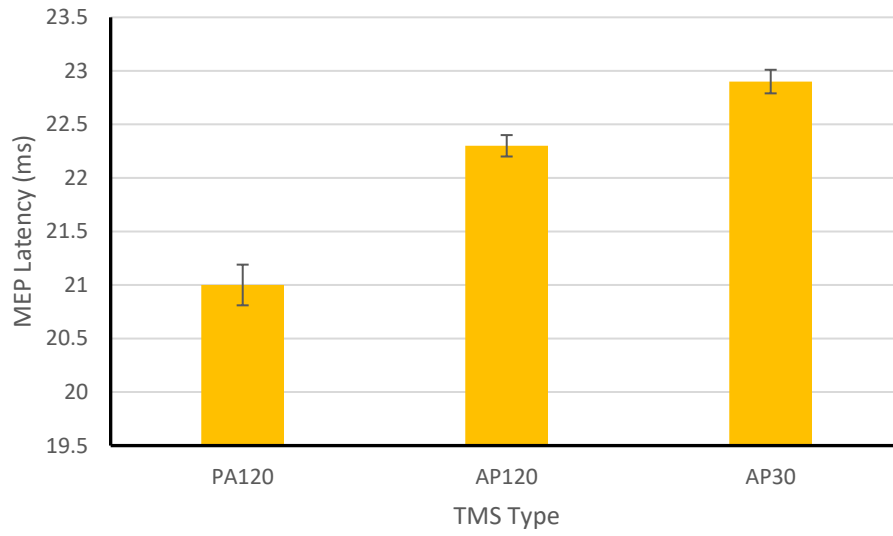
Figure 8 - MEP Latency (ms) vs TMS Type. MEP Latency represents the amount of time between the peripheral stimulus and TMS stimulus. The error bars represent the standard error mean of the dataset.
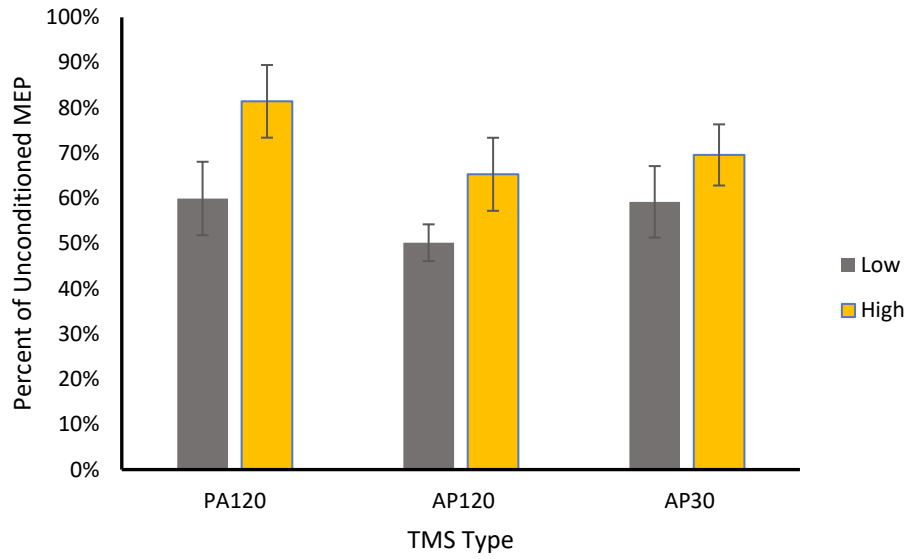
Figure 99 - Percent of Unconditioned MEP vs. TMS Type. Percent of Unconditioned MEP represents the average conditioned MEP value divided by the average amount of MEP produced in the unconditioned trials. The error bars represent the standard error mean of the dataset.

4.4 Effect of Frequency by Load and TMS Type on SAI

The modulatory effect of different frequencies was investigated using separate linear mixed

models that included the categorical variables Load (Low, High) and TMS Type (PA120,

AP120, AP30) as well as the continuous factor ERSP amplitude for each frequency bin (Theta,

Alpha, Low Beta, High Beta, Gamma) and electrode site (CP3, FCz).

4.4.1 The interaction between ERSP Amplitude at the CP3 electrode site, Memory Load

and TMS Configuration

Figure 10 depicts example spectrograms from a single participant for low and high-load working

memory trials at electrode site CP3. The spectrogram is the average across all trials for that

participant.

For the mixed model including Theta ERSP amplitude, there were no significant main

effects for Load $[F_{1,62} = 2.13, \ p = \ 0.15, \ \eta_p^2 = 0.03 \ ]$, TMS Type $[F_{1,58} \ = \ 0.10, p = $

$0.37, \ \eta_p^2 = 0.03]$,

or ERSP Amplitude $[F_{1,56} = 0.51, p = 0.48, \ \eta_p^2 = 9.02\mathrm{e}^{-03}]$, or two-way interactions for Load

x TMS Type $[F_{1,56} = 1.66, p = 0.20, \ \eta_p^2 = 0.06 \ ]$, Load x ERSP Amplitude $[F_{1,62} = \ 0.69, p = $

$0.20, \ \eta_p^2 = 0.03 \ ]$, TMS Type x ERSP Amplitude $[F_{1,58} = 0.87, p = 0.42, \ \eta_p^2 = 0.03 \ ]$ or the

three-way interactions Load x TMS Type x ERSP Amplitude $[F_{1,56} = 1.57, p = 0.22, \ \eta_p^2 = $

$0.05 \ ]$.
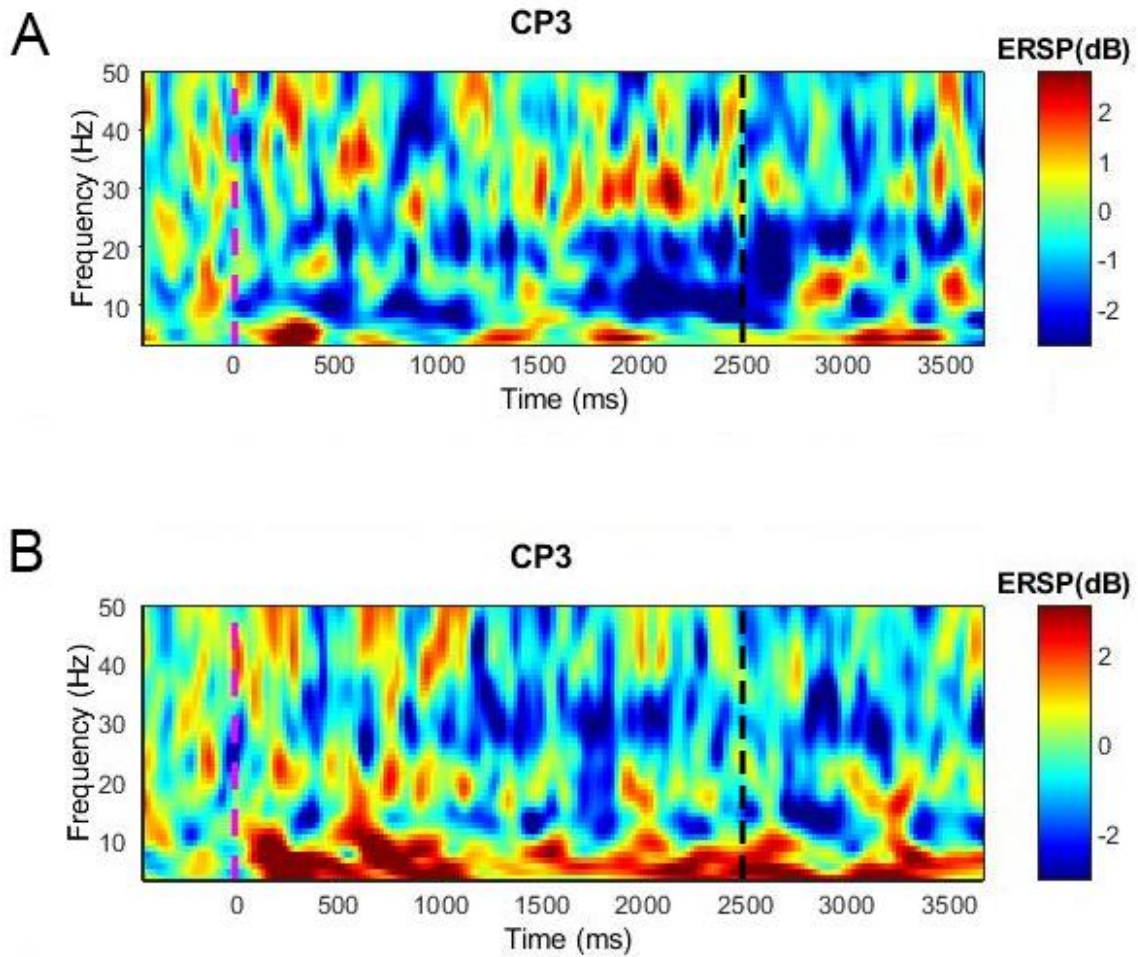
Figure 100 - Sample participant spectrogram at CP3 electrode for A: Low working memory load B: High working memory load. The purple dotted line represents the end of the pretrial phase. The black dotted line marks the start of the maintenance window.

For Alpha ERSP amplitude there was a significant effect of Load $[F_{1,58} = 9.24, p = 0.0035, \eta_p^2 = 0.14;$ Low $= 0.565\% \pm 0.6,$ mean $\pm$ standard error, High $= 0.773\% \pm 0.06]$ and a significant Load x ERSP Amplitude interaction $[F_{1,58} = 98.38, p = 0.0054, \eta_p^2 = 0.13;$ Low $= 1.20\% \pm 0.6,$ mean $\pm$ standard error, High $= 0.773\% \pm 0.06]$. None of the other main effects of TMS Type $[F_{1,57} = 0.65, p = 0.53, \eta_p^2 = 0.02]$ and ERSP Amplitude $[F_{1,56} = 0.52, p = 0.47, \eta_p^2 = 9.02e^{-03}]$ or interactions Load x TMS Type $[F_{1,59} = 1.60, p = 0.21, \eta_p^2 = 0.05]$, TMS Type x ERSP Amplitude $[F_{1,57} = 0.69, p = 0.51, \eta_p^2 = 0.02]$, Load x TMS Type x ERSP Amplitude $[F_{1,59} = 1.52, p = 0.23, \eta_p^2 = 0.05]$, reached significance. The significant effect of Load was driven by a 16.8% decrease in SAI from Low to High Load. The significant effect of Load x ERSP Amplitude interaction was driven by a decrease of 31.5% in ERSP amplitude from Low to High Load see Figure 1.

For Low Beta ERSP amplitude, there were no significant main effects for Load: $[F_{1,60} = 0.46, p = 0.50, \eta_p^2 = 7.52e^{-03}]$, TMS Type $[F_{1,60} = 1.20, p = 0.31, \eta_p^2 = 0.04]$, ERSP Amplitude $[F_{1,58} = 0.07, p = 0.80, \eta_p^2 = 1.12e^{-03}]$, two-way interactions Load x TMS Type $[F_{1,56} = 2.03, p = 0.14, \eta_p^2 = 0.07]$, Load x ERSP Amplitude $[F_{1,60} = 0.28, p = 0.60, \eta_p^2 = 4.67e^{-03}]$, TMS Type x ERSP Amplitude $[F_{1,60} = 1.12, p = 0.33, \eta_p^2 = 0.04]$ or the three-way interactions Load x TMS Type x ERSP Amplitude $[F_{1,56} = 1.95, p = 0.15, \eta_p^2 = 0.06]$. For High Beta ERSP amplitude there was a strong trend for a main effect of ERSP Amplitude $[F_{1,59} = 3.51, p = 0.066, \eta_p^2 = 0.06]$ None of the other main effects were significant Load $[F_{1,56} = 0.42, p = 0.52, \eta_p^2 = 7.43e^{-03}]$, TMS Type $[F_{1,60} = 0.42, p = 0.66 \ \eta_p^2 = 0.01]$. None of the two-way Load x TMS Type $[F_{1,57} = 0.47, p = 0.63, \eta_p^2 = 0.02]$, Load x ERSP
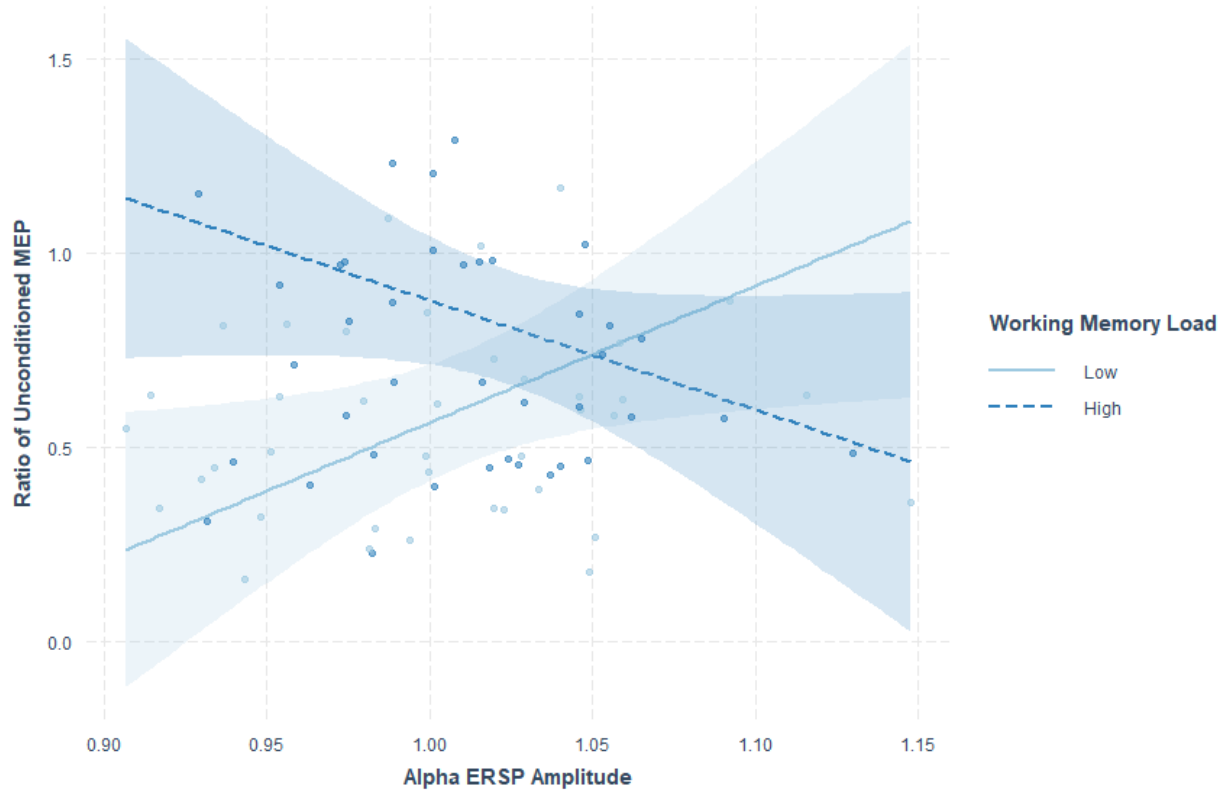
Figure 11 - Ratio of Unconditioned MEP by Alpha ERSP Amplitude at electrode CP3 quantified during the low and high working memory load tasks

Amplitude $\left[F_{1,56} = 0.58, \text{p} = 0.45, \eta_p^2 = 0.01\right]$, TMS Type x ERSP Amplitude $\left[F_{1,60} = 0.37, \text{p} = 0.70, \eta_p^2 = 0.01\right]$, or the three-way Load x TMS Type x ERSP Amplitude $\left[F_{1,57} = 0.43, \text{p} = 0.65, \eta_p^2 = 0.01\right]$, interactions were significant.

For Gamma ERSP amplitude there were no significant main effects for Load $\left[F_{1,59} = 0.0035, \text{p} = 0.95, \eta_p^2 = 5.87\text{e}^{-05}\right]$, TMS Type $\left[F_{1,57} = 0.09, \text{p} = 0.91, \eta_p^2 = 3.17\text{e}^{-03}\right]$, or ERSP Amplitude $\left[F_{1,59} = 2.64, \text{p} = 0.11, \eta_p^2 = 0.04\right]$. None of the two-way Load x TMS Type $\left[F_{1,58} = 1.98, \text{p} = 0.15, \eta_p^2 = 0.06\right]$, Load x ERSP Amplitude $\left[F_{1,57} = 0.023, \text{p} = 0.88, \eta_p^2 = 3.92\text{e}^{-04}\right]$, TMS Type x ERSP Amplitude $\left[F_{1,57} = 0.13, \text{p} = 0.88, \eta_p^2 = 4.55\text{e}^{-03}\right]$, or the three-way Load x TMS Type x ERSP Amplitude $\left[F_{1,60} = 1.81, \text{p} = 0.17, \eta_p^2 = 0.06\right]$, interactions were significant. See **Error! Reference source not found.**0.

4.4.2 The interaction between ERSP Amplitude at the FCz electrode site, Memory Load and TMS Configuration

Figure 12 depicts example spectrograms from a single participant for low and high-load working memory trials at electrode site FCz. The spectrogram is the average across all trials for that participant.

For Theta ERSP amplitude, there were no significant main effects for Load $\left[F_{1,59} = 1.47, \text{p} = 0.23, \eta_p^2 = 0.02\right]$, TMS Type $\left[F_{1,59} = 0.58, \text{p} = 0.56, \eta_p^2 = 0.02\right]$, or ERSP Amplitude $\left[F_{1,58} = 0.04, \text{p} = 0.83, \eta_p^2 = 7.66\text{e}^{-04}\right]$, or two-way interactions for Load x TMS Type $\left[F_{1,58} = 0.41, \text{p} = 0.67, \eta_p^2 = 0.01\right]$, Load x ERSP Amplitude $\left[F_{1,59} = 1.89, \text{p} = 0.17, \eta_p^2 = 0.03\right]$, TMS Type x ERSP Amplitude $\left[F_{1,58} = 0.48, \text{p} = 0.62, \eta_p^2 = 0.02\right]$ or the
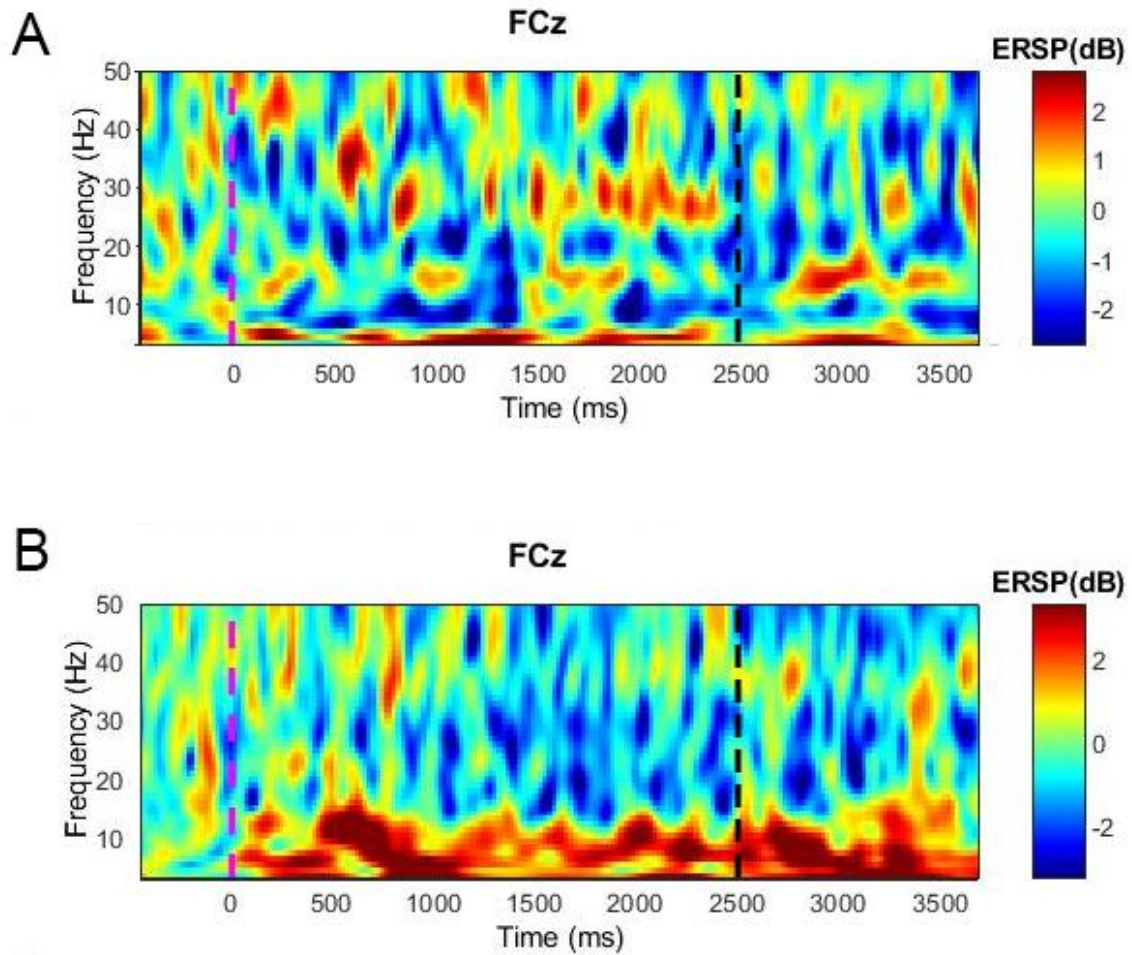
Figure 11- Sample participant spectrogram at FCz electrode for A: Low working memory load B: High working memory load. The purple dotted line represents the end of the pretrial phase. The black dotted line marks the start of the maintenance window.
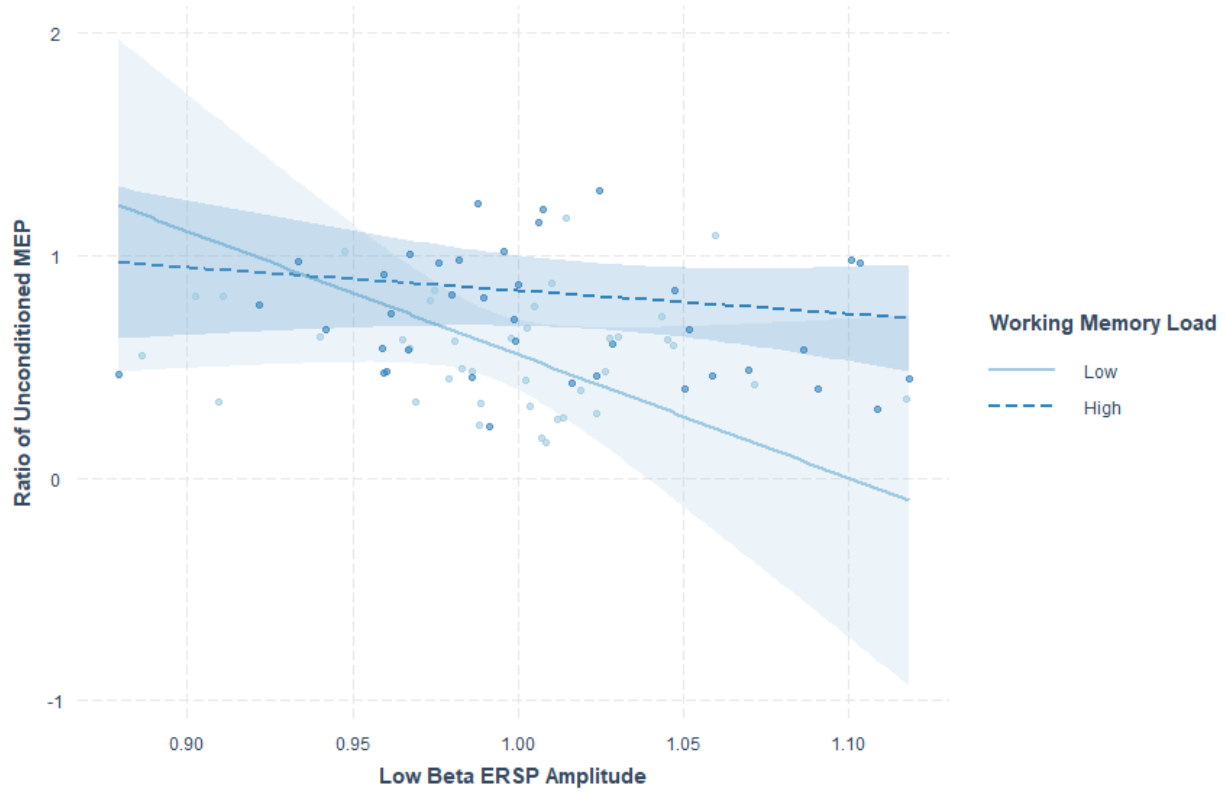
Figure 123- Ratio of Unconditioned MEP by Low Beta ERSP Amplitude at electrode FCz

quantified during the low and high working memory load tasks

three-way interactions Load x TMS Type x ERSP Amplitude $[F_{1,58} = 0.45, p = 0.64, \eta_p^2 = 0.02]$.

For Alpha ERSP amplitude there were no significant main effects for Load $[F_{1,57} = 1.27, p = 0.26, \eta_p^2 = 0.02]$, TMS Type $[F_{1,58} = 0.61, p = 0.54, \eta_p^2 = 0.02]$, or ERSP Amplitude $[F_{1,57} = 0.44, p = 0.51, \eta_p^2 = 7.56e^{-03}]$, or two-way interactions for Load x TMS Type $[F_{1,60} = 0.19, p = 0.83, \eta_p^2 = 6.21e^{-03}]$, Load x ERSP Amplitude $[F_{1,58} = 11.67, p = 0.20, \eta_p^2 = 0.03]$, TMS Type x ERSP Amplitude $[F_{1,58} = 0.69, p = 0.51, \eta_p^2 = 0.02]$ or the three-way interactions Load x TMS Type x ERSP Amplitude $[F_{1,60} = 0.21, p = 0.81, \eta_p^2 = 6.87e^{-03}]$.

For Low Beta ERSP amplitude there was a significant effect of ERSP Amplitude $[F_{1,57} = 4.59, p = 0.036, \eta_p^2 = 0.06]$ and a significant Load x ERSP Amplitude interaction $[F_{1,57} = 0.057, p = 0.049, \eta_p^2 = 0.07;$ Low $= -2.87\% \pm 1.2,$ mean $\pm$ standard error, High $= -0.07\% \pm 0.7]$. There was also a strong trend for a significant main effect of Load $[F_{1,57} = 3.55, p = 0.064, \eta_p^2 = 0.06]$. There was no main effect for TMS Type $[F_{1,57} = 0.48, p = 0.63, \eta_p^2 = 0.04]$ or the interactions Load x TMS Type $[F_{1,57} = 1.33, p = 0.27, \eta_p^2 = 0.04]$, TMS Type x ERSP Amplitude $[F_{1,57} = 0.47, p = 0.63, \eta_p^2 = 0.02]$ or Load x TMS Type x ERSP Amplitude $[F_{1,59} = 1.52, p = 0.23, \eta_p^2 = 0.05]$. The significant effect of Load x ERSP Amplitude interaction was driven by a decrease of 2.8% in ERSP amplitude from Low to High Load. See Figure 123.

For High Beta ERSP amplitude there were no significant main effects for Load $[F_{1,60} = 0.48, p = 0.49, \eta_p^2 = 8.01e^{-03}]$, TMS Type $[F_{1,59} = 0.92, p = 0.41, \eta_p^2 = 0.03]$, or ERSP Amplitude $[F_{1,57} = 0.04, p = 0.84, \eta_p^2 = 7.33e^{-04}]$, or two-way interactions for Load x TMS Type $[F_{1,60} = 0.05, p = 0.95, \eta_p^2 = 1.81e^{-03}]$, Load x ERSP Amplitude $[F_{1,60} = 0.67, p = 0.42, \eta_p^2 = 0.01]$, TMS Type x ERSP Amplitude $[F_{1,59} = 0.81, p = 0.45, \eta_p^2 = 0.03]$ or the three-way interactions Load x TMS Type x ERSP Amplitude $[F_{1,58} = 0.03, p = 0.97, \eta_p^2 = 1.17e^{-03}]$.

For Gamma ERSP amplitude there were no significant main effects for Load $[F_{1,55} = 0.31, p = 0.58, \eta_p^2 = 5.64e^{-03}]$, TMS Type $[F_{1,58} = 0.06, p = 0.94, \eta_p^2 = 2.16e^{-03}]$, or ERSP Amplitude $[F_{1,59} = 0.03, p = 0.86, \eta_p^2 = 5.00e^{-04}]$, or two-way interactions for Load x TMS Type $[F_{1,58} = 0.42, p = 0.66, \eta_p^2 = 0.01]$, Load x ERSP Amplitude $[F_{1,55} = 0.57, p = 0.45, \eta_p^2 = 0.01]$, TMS Type x ERSP Amplitude $[F_{1,58} = 0.04, p = 0.97, \eta_p^2 = 1.22e^{-03}]$ or the three-way interactions Load x TMS Type x ERSP Amplitude $[F_{1,58} = 0.39, p = 0.68, \eta_p^2 = 0.01]$.

5.0 DISCUSSION

This study had two main goals. First, to assess the effect of working memory load on sensorimotor integration, as indexed by SAI. Second, to evaluate the modulatory effect of different EEG frequencies on the impact of working memory load on SAI. Similar to past work (Suzuki & Meehan, 2018), SAI was reduced under a high verbal working memory load across both PA and AP sensorimotor circuits. Parietal alpha ERSP amplitude appeared to shape the working memory effect on SAI elicited by all TMS current types. Under low load, the amount of SAI increased with alpha desynchronization. In contrast, increased alpha synchronization was associated with greater SAI under high working memory loads. Frontal Low beta ERSP amplitude also influenced SAI elicited by all the TMS current types. High levels of low beta ERSP amplitude yielded less SAI under a low working memory load. However, low beta ERSP amplitude did not modulate SAI under high loads. Finally, high levels of high beta ERSP amplitude over the sensorimotor cortex were associated with lower levels of SAI regardless of working memory load and TMS current type.

On the surface, the results of the current study mirror past work (Suzuki & Meehan, 2018) using traditional TMS. Suzuki and Meehan (2018) found that both PA and AP SAI decreased as verbal working memory load increased. However, there is a major divergence between the current study and work by Suzuki and Meehan (2018). Suzuki and Meehan (2018) used PA and AP current with a single, fixed duration of ~72 µs. In contrast, the current study employed PA current with a pulse width of 120 µs and AP with a short 30 µs or long 120 µs pulse width. The intermediate duration of ~72 µs likely recruits neuron populations from a combination of long and short-duration circuits (Hannah & Rothwell, 2017). Based on previous work, it also appears that AP30 current, is functionally distinct from longer TMS pulse durations (D'Ostilio et al.,

2016; Hannah & Rothwell, 2017). The current study's results, however, run counter to the idea that the AP30 stimulus appears to engage unique neural circuits, as working memory decreased both AP120 and AP30 SAI.

The lack of dissociation between AP120 and AP30 current seen in the current results could be due to a masking effect of several elements. One element could be the small sample size which was only able to detect a magnitude difference rather than a dissociation in the response of AP120 and AP30 to working memory load. The effect of 0.02 suggests that there is not evidence for a meaningful difference in the magnitude of the reduction in SAI induced by high working memory load across the different TMS currents.

Another explanation for the lack of dissociated between AP120 and AP30 could be that the current study assessed SAI during a working memory task and not at relative rest like the previously mentioned cTMS studies (D'Ostilio et al., 2016; Hannah & Rothwell, 2017). Whereas, the current study has subjects engage their verbal working memory, placing a much greater load on the subject's executive functioning. The difference in the cognitive state between relative rest and being placed under executive load could potentially be what is resulting in the loss or alteration of whatever makes AP30 distinct. It appears that SAI results from multiple converging sensorimotor loops and circuits and not a single circuit or input (D'Ostilio et al., 2016; Hannah & Rothwell, 2017; Turco et al., 2018b). Based on current results, it appears that the introduction of executive load likely only manipulates common inputs across all current types. This means if unique inputs, such as the cerebellum are not modulated, no distinction will be seen across any of the circuits (Hannah & Rothwell, 2017).

A potential way of explaining the common SAI response seen across circuits is to look at the working memory task's impact on an element, such as I waves. Regardless of changes in

TMS direction or duration, the MEP produced is a product of some combination of I-waves converging on the corticospinal output neuron in the motor cortex (Di Lazzaro et al., 2012; Hannah & Rothwell, 2017). Although, the sequence of I-waves elicited by the TMS stimulus varies depending on the stimulus's current direction and pulse width (Di Lazzaro et al., 2012). The timings of the I-waves relative to an MEP elicited by directly stimulating the CSN itself reflect the unique subset of interneurons in the motor cortex that TMS recruits. In turn, SAI quantified using different combinations of current direction and pulse width can provide information about the unique physical and functional properties of the afferent information projected to each subset of interneurons.

Regarding I waves, one possible explanation for the common SAI effect, would be that all three stimulus types are recruiting the same I waves. There is normally a distinction between the two current directions, as PA primarily elicits early I1- and I2-waves, whereas AP primarily elicits later I3- and I4-waves (Di Lazzaro et al., 2001). However, past work has shown that this distinction can be eliminated by providing PA stimulus at higher stimulation intensities, causing PA current to evoke I3- and I4-waves (Di Lazzaro et al., 2001). The production of later I waves by PA current demonstrates that it is possible, given the right conditions, to cause differences across TMS stimulus types to be eliminated, resulting in the same transsynaptic projections being used. The uniformity in SAI response seen in the current study is unlikely to be due to this specific phenomenon. The MEPs elicited to provoke that PA response were much greater (≥ 2 mV) than those used in the current study (~1 mV) (Di Lazzaro et al., 2001). The stimulus levels used by the current study produced a distinction between I waves recruited by PA and AP stimulus, which is reflected by the increasing MEP onset latency from PA120 to AP120 to AP30 current.

The conditions that produce the differences seen across current direction and duration, appear to depend on the activity levels of specific brain regions at the time of stimulation (Hamada et al., 2014; Hannah & Rothwell, 2017; Spampinato et al., 2020). The current study demonstrates that the activity levels of particular brain regions also appear to influence SAI when no distinction is present. The present study found that the responsiveness of SAI to working memory load was shaped by frontal alpha ERSP amplitude. A previous study which also found a reduction in SAI with increased verbal working memory load found that there was a reduction in the parietal N20-P25 SEP amplitude (Suzuki & Meehan, 2018). Therefore, the relationship seen in the current study between parietal EEG activity and SAI, is consistent with past work, helping prove that S1 projections i.e., the N20-P25 SEP, play a critical part in SAI production (Dancey et al., 2016; Suzuki & Meehan, 2018). Although it should be noted that the parietal N20-P25 data was from a separate sample, so they were not able to produce a direct correlation (Suzuki & Meehan, 2018). That being said, other past work has proven the existence of a direct correlation between the parietal N20-P25 SEP and PA SAI magnitude (Bailey et al., 2016).

The parietal ERSP amplitude changes for the alpha frequency seen in the current study have not been investigated previously. However, past work has shown that there is an inverse relationship between parietal alpha ERSP amplitude and visual encoding tasks (Pfurtscheller et al., 1996). During visual encoding tasks, such as reading, parietal alpha synchronization increases in sensorimotor areas (Pfurtscheller et al., 1996). This supports the idea that the alpha frequency is associated with cortical idling. The afferent information from the resting hand is not critical during reading. Therefore, the region is put into an 'idling state', freeing up resources for the regions relevant to the task (Pfurtscheller et al., 1996).

Another consideration regarding the results of the current study is the presence of a peripheral stimulus. The additional processing of the peripheral stimulus could lead to differences in the overall brain state, resulting in differences in the alpha ERSP signal. The impact of the peripheral stimulus on the alpha ERSP amplitude is difficult to prove since the ERSP amplitude result is a ratio of conditioned ERSP/unconditioned ERSP. Therefore, solely using the ERSP ratio, one cannot determine whether the additional processing of the peripheral stimulus is leading to a significant state change in the sensorimotor neurons and having an impact on the overall ERSP signal. That being said, any impact that the peripheral stimulus would have on the ERSP measures would be minimal, as the window of time being studied ends just prior to the onset of the peripheral stimulus. Therefore, since the ERSP is an average of the maintenance window prior to TMS stimulus, the peripheral stimulus should have little impact on the overall measure.

Parietal alpha desynchronization has also specifically been linked to working memory, with these working memory studies supporting the idea that parietal alpha synchronization is associated with cortical idling and the reduction of distractions. A positive correlation had been established between alpha desynchronization and memory performance (Klimesch, 1999). A previous study has also found that like the current study, during a Sternberg task, changes in alpha band activity were seen during the maintenance window (Jensen et al., 2002). It was also found that there was a graded effect depending on the number of items being stored, with parietal alpha synchronization increasing with load, as well as, progressively increasing across the maintenance window (Jensen et al., 2002).

Alpha synchronization, representing distraction and increasing with working load also follows the traditional concept of load theory, where increased executive load results in increased

distractions (Lavie et al., 2004). According to load theory, increased executive load disrupts late selection processes, leading to greater distraction (Lavie et al., 2004). The current findings that at low working memory load, greater amounts of alpha synchronization result in decreased SAI, is consistent with load theory. The greater alpha ERSP amplitude reflects a suppression or gating of sensory afference that, in turn, reduces SAI as there is a weaker projection of afference to M1. However, this is not the case at high working memory load. At high working memory load, greater amounts of alpha synchronization were associated with lower levels of SAI. The effect of alpha synchronization under high working memory loads may reflect the interaction between working memory and cortical idling. As noted, increasing working memory load itself, enhances alpha synchronization during memory maintenance (Jensen et al., 2002). Therefore, the increased alpha synchronization under high load may reflect individuals better able to manage the increased working memory load and therefore, less gating of irrelevant information may occur. In contrast, those individuals who demonstrate less alpha synchronization may be struggling to manage the increased working memory load, placing a greater premium on reducing potential distraction by task-irrelevant information. The former would lead to greater SAI despite the increased synchronization as these individuals have excess cognitive resources available and do not gate the irrelevant somatosensory afference as extensively. In contrast, the latter would lead to less SAI as working memory is not as efficient and task-irrelevant somatosensory afference is gated to a greater extent leading to a reduction in afferent projection to M1, and less SAI.

Overall, alpha synchronization appears to be a critical part of a concept known as cortical idling, which allows for the restriction of distractions and unwanted movement during cognitive tasks that engage executive functioning. However, the current results reveal that under more

intensive levels of executive load, this relationship breaks down. Resulting in impairment of the

ability to adequately modulate alpha synchronization, leading to the opposite effect of greater

alpha synchronization resulting in greater SAI under high working memory load. Due to the

uniformity in direction of the SAI response in the current study, alpha synchronization appears to

impact all of the sensorimotor circuits studied in the same way.

ERSP amplitude for the frontal low beta frequency supports previous results. A previous

study which also found a reduction in SAI with increased verbal working memory load, using a

similar Sternberg working memory task, found that there was an increase in the frontal P20-N30

amplitude (Suzuki & Meehan, 2018). Therefore, the relationship seen in the current study

between frontal EEG activity and SAI, is consistent with past work, helping prove that SMA

projections i.e., the P20-N30 amplitude, play a critical part in SAI production (Kaňovský et al.,

2003; Suzuki & Meehan, 2018). This potential SMA relationship means that the frontal low beta

results of the current study could relate to movement planning and execution. The SMA is

known to be involved in the planning and execution of complex movements of the contralateral

extremities (Kennerley et al., 2004). Previous work has also shown that changes in low beta EEG

frequency, specifically, low beta desynchronization, could be a contributing factor to the

execution of movement (Andres et al., 1999; Fischer et al., 2016; Puzzo et al., 2013; Puzzo et al.,

2011).

While the current study is not explicitly studying movement initiation, a slight

contraction of the FDI was required to lower the TMS stimulus intensity required to elicit an

MEP of sufficient size to assess SAI, especially for the AP30 current. Due to the contraction, the

current study's result that during low working memory load, low levels of low beta ERSP

amplitude yielded greater SAI, indirectly follows the trend of low beta desynchronization

correlating with movement execution. The reasoning behind the relationship regarding low beta ERSP amplitude only being present during low working memory load is likely due to the lower executive load on the subject. During high working memory load, there is likely too much executive load being placed on the system. Which leaves no additional cognitive resources to be devoted to maintenance of the muscle contraction. Whereas, at lower executive loads, the level of difficulty for each subject is much more variable. Resulting in a greater difference in excess cognitive resources to dedicate to the muscle contraction, causing the trend we currently see. In this way, frontal low beta ERSP changes could be thought of as directing cognitive resources towards motor performance, but differences can only be seen if there are adequate cognitive resources available. Previous work supports the theory of cognitive resource allocation by showing that reductions in low beta synchronization reflect increased focus on movement execution (Andres et al., 1999; Fischer et al., 2016; Puzzo et al., 2011). The opposite effect has also been found, further supporting the allocation theory. Increased movement confidence, and therefore lower executive load, resulted in increased low beta synchronization over the SMA (Fischer et al., 2016).

The present study's finding of ERSP amplitude at high beta frequency influencing SAI across working memory load is likely the most straightforward yet the hardest to support, as very few studies distinguish between low and high beta frequencies. The same trend of high levels of low beta ERSP amplitude yielding less SAI, is consistent for both high and low working memory loads. That consistency makes it likely the case that high beta frequency at S1 is responsible for helping set the baseline level of SAI. While these studies don't necessarily differentiate between high and low beta, there is previous work that supports the idea that beta frequencies are associated with assisting in maintaining a steady state of the motor system and are believed to

57

represent the average or 'status quo' (Engel & Fries, 2010; Heinrichs-Graham et al., 2014). The concept of beta frequencies being associated with maintenance of sensorimotor control, is further supported by previous work which has found increased beta desynchronization concerning maintaining muscle contraction (Engel & Fries, 2010; Pfurtscheller & Lopes da Silva, 1999). Furthermore, when taken to its extreme, as seen in Parkinson's disease, there is an abnormal enhancement of activity in the beta frequency (Engel & Fries, 2010). The abnormal enhancement if taken too far can result in an unhealthy persistence of the status quo, causing the deterioration of flexible behavioural and cognitive control (Engel & Fries, 2010).

In summary, the current study's findings expand on past work in several ways. One of the most notable is using multiple TMS stimulus durations. The current study added to previous findings that both PA and AP SAI decreased as verbal working memory load increased, demonstrating that a reduction in SAI is seen regardless of stimulus direction or duration. Based on previous results, it was expected that there would be more of a difference in SAI across the different TMS stimulus types. A potential reason for the lack of difference in SAI could be that changes in executive load through the working memory task does not adequately engage unique sensorimotor circuits for a particular stimulus type. That being said, the ERSP changes seen in the current study could explain some potential sources of sensorimotor inputs, and the impact that they have on sensorimotor control. The changes in parietal alpha ERSP amplitude likely relate to cortical idling at low working memory loads. A breakdown of executive functioning likely occurs at higher working memory loads, causing parietal alpha ERSP amplitude to no longer be representative of cortical idling. Frontal low beta ERSP amplitude is likely related to movement execution and the amount of focus being applied to a movement task. Under low working memory load, frontal low beta ERSP amplitude has a negative correlation with SAI,

58

which is not present at high working memory loads. The lack of relationship at high load is likely

due to there being less of a difference in difficulty across participants. The lack of difference

resulting in no relationship due to the similarity of results. The last of the major ERSP changes,

parietal high beta ERSP amplitude appears to assist in establishing baseline levels of SAI.

6.0 LIMITATIONS

The current study has several limitations which should be acknowledged. The primary limitation of the current study was that it was underpowered. There were restrictions regarding time and availability of participants, due to the Covid-19 restrictions and lockdown, causing not as many participants to be recruited as normal. Additionally, subjects had to be removed from the dataset, due to either not being able to achieve an adequate 1 mV MEP for AP30 stimulation or getting a score of <60% during the working memory task. The combination of covid restrictions and the further removal of subjects resulted in the overall sample size of the study being smaller than required to be confident of avoiding Type II statistical errors. Inspection of effect sizes suggest that the chances of making a Type II error are relatively small. None of the effect sizes are large enough to reach a significant outcome even with the smaller sample size.

A second limitation is that the working memory task chosen was shown to have similar effects across PA and AP current of ~72 μs. In contrast, PA and AP SAI have been dissociated using a visual detection task emphasizing sustained attention (Mirdamadi et al. 2018). The choice of the working memory task was intentional to determine whether the common effect of working memory across PA and AP current was driven by AP120 circuits rather than AP30 circuits, both of which may be indiscriminately recruited by the 72 μs stimulus. The current results suggest that there are commonalities across the AP120 and AP30 circuits in response to working memory load. These commonalities do not preclude the possibility that AP120 and AP30 have unique afferent inputs as well. However, the unique afferent inputs, and the oscillatory activity reflecting these inputs, were not evident with the working memory task. It is possible AP120 and AP30 may be dissociated by the perceptual load of a visual detection task and associate with oscillatory activity in unique frequency bands at distinct electrode sites.

Alternatively, the unique relationships between AP30 SAI and oscillatory activity could be studied by measuring both before and after neuromodulation of various cortical or subcortical structures. For example, cerebellar modulation has been demonstrated to preferentially modulate AP30 sensorimotor circuits (Hannah & Rothwell 2017). The specificity of cerebellar modulation could unmask changes in cortical oscillatory activity that reflect the specific cerebellar mediated modulation of the AP30 sensorimotor circuit in M1.

A third limitation is that the two electrodes used for the ERSP measures were chosen a priori. Due to choosing the electrodes beforehand, there are potential significant relationships involving other electrodes being missed. Analyzing the EEG data after data collection and then, determining which electrodes to focus on, would have avoided missing any potential other relationships. However, it would have taken a substantial amount of extra time to analyze each electrode. As stated previously, due to extenuating circumstances, time was not available to do such an analysis. Furthermore, the electrodes that were chosen, had substantial evidence from previous work suggesting their involvement in the sensorimotor circuits being studied.

7.0 CONCEPTUAL MODEL REVISED

My updated conceptual model (see Figure 14) still supports the idea that there are distinct sensorimotor inputs informing SAI across different current types. However, unlike the previous model, the current model gives a greater amount of common inputs, in addition to distinct ones. One of the known common influences across all of the inputs is that an increase in working memory load, results in decreased SAI for all stimulus types. This suggests that the circuits for all stimulus types likely have an input from S1, the proposed generator of the N20 SEP (Dancey et al., 2016). The N20 generator was chosen because the N20 has been associated with changes in working memory load in previous studies and was believed to be a source of the distinction regarding AP30 stimulation (Suzuki & Meehan, 2018). Which is also in line with the current study's findings of parietal alpha synchronization being influenced by working memory load. Other common influences across all of the circuits are likely thalamus, premotor areas and basal ganglia. These regions were chosen due to their relationship with the frontal N30, which is believed to influence a cortico-thalamic loop containing those areas specific areas (Cebolla et al., 2011). Which is also in line with the current study's findings of frontal low beta being influenced by working memory load.

There are also several distinctions across the circuits. The previous model (see Figure 1) did not differentiate between the specific M1 layers each circuit inputs to, however, since my previous model, a recent modeling study has shed light on the specific layers that may be involved (Aberra et al., 2020), see Figure 14. The PA120 circuit is likely directly stimulating the terminals of L5 pyramidal neurons within M1 monosynaptically (Aberra et al., 2020). Whereas, the two AP circuits activate rostral M1 or pre-motor pyramidal cells polysynaptically
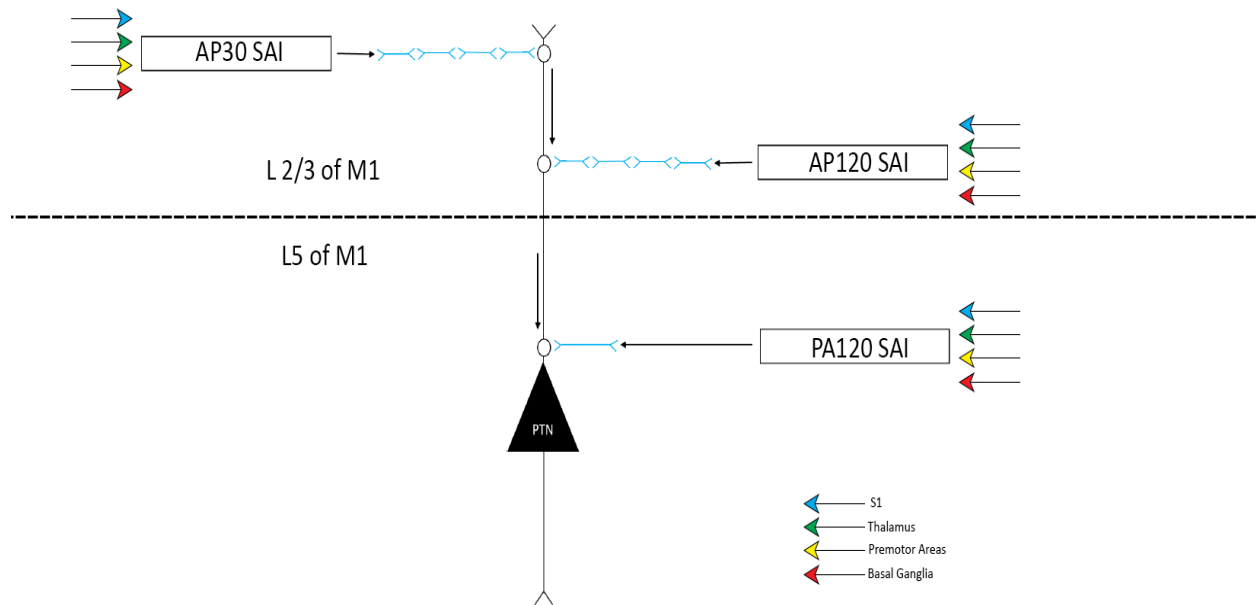
Figure 13- Revised Conceptual Model. It depicts the pathways of the sensorimotor signal for each TMS current direction into the PTN. The blue lines indicate neurons. The coloured arrows represent individual incoming inputs from others brain regions. The dashed line separates brain regions.

(Aberra et al., 2020). Furthermore, the distinction is made that specifically AP120 likely activates rostral M1, whereas AP30 likely recruits pre-motor cells. The distinction between AP stimuli was made since the current study, along with previous work has shown that AP30 stimulus typically occurs later than AP120. Therefore, its input is likely located further away (Hannah & Rothwell, 2017). Although the current studies offer limited support for a differential response to working memory, a AP120-AP30 distinction is supported by the fact that the AP120 circuit appears to be more functionally similar to the PA120 circuit than it is to the AP30 circuit (Hannah & Rothwell, 2017).

8.0 FUTURE DIRECTIONS

The future directions provided above specifically address the current study's limitations. However, the current study also highlights several other future directions with regard to identifying the origin of sensorimotor circuits and improving our understanding of the sensorimotor system.

While the verbal working memory task used in the current study does not differentiate between circuits, it can still be beneficial to study other elements of the working memory task. One such element would be changing the working memory task's timing window. The current study focused on the maintenance window in its entirety. Future studies could follow a similar process but look at a narrower band of the maintenance window, closer to the TMS stimulus. This could provide clearer information regarding the state of the brain immediately prior to TMS stimulus. Therefore, providing a better understanding as to the likely brain regions that are active as the stimulus is occurring and how the regions inform sensorimotor integration.

Furthermore, instead of the maintenance window, the encoding phase of the working memory task could be studied. Studying the encoding phase would provide greater insight into the impact of working memory on the sensorimotor process. Little is known about the impact of the quality of encoding or ability to encode information on SAI and should be studied further.

Another future direction would be further examination of the different sensorimotor circuits through their relationship with SEP measurements. Specifically, the N20 and N30 SEPs as they both have clear links to various sensorimotor processes and sensorimotor loops, as well as, impacting SAI. The best way to do this would likely be to combine online EEG measures with a task such as applying cTMS alongside cerebellar direct current stimulation. Ensuring to choose a task that is known to display differences across circuits. That way you guarantee that a

difference in circuits should be seen, which can then be examined further via changes in the

SEPs. Given the N20 and N30 SEPs link to the sensorimotor system, they may act as markers

when changes are seen across sensorimotor circuits. If they act as markers, that provides

tremendous potential regarding our ability to use SEPs to understand when critical changes occur

in the sensorimotor system. A better understanding of these sensorimotor differences can then

aid in catching and monitoring sensorimotor decline due to illnesses like Parkinson's disease and

support better instruction and training regarding motor tasks.

A final future direction would be to apply the combined cTMS and EEG approach to a

more functional motor task. A promising task would be similar to one done previously in our

lab, which presents a sequence to the participant, requiring them to press a series of keys on a

keypad in the presented order. Using such a task would allow for studying the execution of the

movement and the processing of the motor commands. While similar tasks have been studied

previously, it is often only done with TMS or EEG exclusively, not in tandem. The ability to

directly correlate brain region activity to TMS response during such a task is novel. Allowing for

a greater understanding of the inputs involved during sensorimotor integration. The combination

of TMS and EEG, as mentioned previously, also allows for potential markers of changes in the

sensorimotor system to be found, likely in the form of SEPs.

9.0 CONCLUSION

The current study demonstrates the influence of executive load on sensorimotor integration. Increases in working memory load during a verbal working memory task resulted in reductions in SAI across both PA and AP circuits. The first hypothesis, that with an increase in working memory load, there would be a decrease SAI in AP120 and PA120, but an increase in AP30 SAI, was partially supported. There was a decrease in SAI for AP120 and PA120, but a decrease was also seen for AP30. Overall, working memory appears to have a similar directional effect on sensorimotor integration. The directional consistency in SAI response implies at least one common input.

The second hypothesis of the study, that unique oscillatory activity would be associated with PA120 and AP120 versus AP30 was not supported. There were relationships found between the amount of SAI produced and changes in ERSP amplitude across working memory load. However, these relationships were consistent across all stimulus types. The consistency in ERSP amplitude changes across stimulus types supports the idea that there are common inputs, across all sensorimotor circuits. The consistency also suggests that verbal working memory results in a reduction of the sensorimotor inputs that make AP30 distinct.

The current study raises questions about and points toward a potential interaction between brain activity in the form of oscillatory frequencies and sensorimotor control. These interactions should be studied further, which could lead to valuable insights regarding the inner workings of sensorimotor control, aiding in the treatment of disorders such as Parkinson's disease.

REFERENCES

Abbruzzese, G., Marchese, R., Buccolieri, A., Gasparetto, B.,& Trompetto, C. (2001).

Abnormalities of sensorimotor integration in focal dystonia: a transcranial magnetic

stimulation study. *Brain,*124(Pt. 3), 537-45. Doi: 10.1093/brain/124.3.537

Aberra, A. S., Wang, B., Grill, W. M., & Peterchev, A. V. (2020). Simulation of transcranial

magnetic stimulation in head model with morphologically-realistic cortical

neurons. *Brain stimulation*, *13*(1), 175-189.

Allison, T., McCarthy, G., Wood, C. C., & Jones, S. J. (1991). Potentials evoked in human and

monkey cerebral cortex by stimulation of the median nerve: a review of scalp and

intracranial recordings. *Brain*, *114*(6), 2465-2503.

Anderson, K. L., Rajagovindan, R., Ghacibeh, G. A., Meador, K. J., & Ding, M. (2010). Theta

oscillations mediate interaction between prefrontal cortex and medial temporal lobe in

human memory. *Cerebral cortex*, *20*(7), 1604-1612.

Andres, F. G., Mima, T., Schulman, A. E., Dichgans, J., Hallett, M., & Gerloff, C. (1999).

Functional coupling of human cortical sensorimotor areas during bimanual skill

acquisition. *Brain*, *122*(5), 855-870.

Asmussen, M. J., Jacobs, M. F., Lee, K. G., Zapallow, C. M., & Nelson, A. J. (2013). Short-

latency afferent inhibition modulation during finger movement. *PLoS One*, *8*(4), e60496.

https://doi.org/10.1371/journal.pone.0060496

Asmussen, M. J., Zapallow, C. M., Jacobs, M. F., Lee, K. G., Tsang, P., & Nelson, A. J. (2014).

Modulation of short-latency afferent inhibition depends on digit and task-relevance. *PLoS

One*, *9*(8), e104807. https://doi.org/10.1371/journal.pone.0104807

Awiszus, F. (2003). TMS and threshold hunting. *Supplements Clinical Neurophysiology,56*, 13-
23. https://doi.org/10.1016/S1567-424X(09)70205-3

Bailey, A. Z., Asmussen, M. J., & Nelson, A. J. (2016). Short-latency afferent inhibition
determined by the sensory afferent volley. *Journal of Neurophysiology*, *116*(2), 637-644.
https://doi.org/10.1152/jn.00276.2016

Başar, E., Başar-Eroğlu, C., Karakaş, S., & Schürmann, M. (1999). Are cognitive processes
manifested in event-related gamma, alpha, theta and delta oscillations in the
EEG?. *Neuroscience letters*, *259*(3), 165-168.

Başar, E., Başar-Eroglu, C., Karakaş, S., & Schürmann, M. (2001). Gamma, alpha, delta, and
theta oscillations govern cognitive processes. *International journal of
psychophysiology*, *39*(2-3), 241-248.

Beres, A. M. (2017). Time is of the essence: A review of electroencephalography (EEG) and
event-related brain potentials (ERPs) in language research. *Applied psychophysiology and
biofeedback*, *42*(4), 247-255.

Berger, D. J., Masciullo, M., Molinari, M., Lacquaniti, F., & d'Avella, A. (2020). Does the
cerebellum shape the spatiotemporal organization of muscle patterns? Insights from
subjects with cerebellar ataxias. *Journal of Neurophysiology*, *123*(5), 1691-1710.

Bikmullina, R., Bäumer, T., Zittel, S., & Münchau, A. (2009). Sensory afferent inhibition within
and between limbs in humans. *Clinical Neurophysiology*, *120*(3), 610-618.
https://doi.org/10.1016/j.clinph.2008.12.003

Bizzi, E., & Ajemian, R. (2020). From motor planning to execution: a sensorimotor loop

   perspective. *Journal of Neurophysiology*, *124*(6), 1815-1823.

Bizzi, E., Tresch, M. C., Saltiel, P., & d'Avella, A. (2000). New perspectives on spinal motor

   systems. *Nature Reviews Neuroscience*, *1*(2), 101-108.

Cebolla, A. M., Palmero-Soler, E., Dan, B., & Cheron, G. (2011). Frontal phasic and oscillatory

   generators of the N30 somatosensory evoked potential. *NeuroImage*, *54*(2), 1297-1306.

Celebi, O., Temuçin, Ç. M., Elibol, B., & Saka, E. (2012). Short latency afferent inhibition in

   Parkinson's disease patients with dementia. *Movement Disorders*, *27*(8), 1052-1055.

   https://doi.org/10.1002/mds.25040

correlates of attentional focusing during finger movements: A fMRI study. *Journal of Motor*

Crochet, S., Lee, S. H., & Petersen, C. C. (2019). Neural circuits for goal-directed sensorimotor

   transformations. *Trends in neurosciences*, *42*(1), 66-77.

Cruikshank, L. C., Singhal, A., Hueppelsheuser, M., & Caplan, J. B. (2012). Theta oscillations

   reflect a putative neural mechanism for human sensorimotor integration. *Journal of*

   Neurophysiology, *107*(1), 65-77.

D'Ostilio, K., Goetz, S. M., Hannah, R., Ciocca, M., Chieffo, R., Chen, J. C. A., Peterchev, A.

   V., & Rothwell, J. C. (2016). Effect of coil orientation on strength–duration time constant

   and I-wave activation with controllable pulse parameter transcranial magnetic

   stimulation. *Clinical Neurophysiology*, *127*(1), 675-683.

   https://doi.org/10.1016/j.clinph.2015.05.017

Da Silva, F. L., Vos, J. E., Mooibroek, J., & Van Rotterdam, A. (1980). Relative contributions of intracortical and thalamo-cortical processes in the generation of alpha rhythms, revealed by partial coherence analysis. *Electroencephalography and clinical neurophysiology*, *50*(5-6), 449-456.

Dancey, E., Murphy, B., Andrew, D., & Yielder, P. (2016). Interactive effect of acute pain and motor learning acquisition on sensorimotor integration and motor learning outcomes. *Journal of neurophysiology*, *116*(5), 2210-2220.

Day, B. L., Dressler, D., Maertens de Noordhout, A. C., Marsden, C. D., Nakashima, K., Rothwell, J. C., & Thompson, P. D. (1989). Electric and magnetic stimulation of human motor cortex: surface EMG and single motor unit responses. *The Journal of Physiology*, *412*(1), 449-473. https://doi.org/10.1113/jphysiol.1989.sp017626

De Pascalis, V., Vecchio, A., & Cirillo, G. (2020). Resting anxiety increases EEG delta–beta correlation: relationships with the reinforcement sensitivity theory personality traits. *Personality and Individual Differences*, *156*, 109796.

Di Lazzaro, V., Oliviero, A., Pilato, F., Saturno, E., Dileone, M., Marra, C., Ghirlanda, S., Ranieri, F., Gainotti, G., & Tonali, P. (2005). Neurophysiological predictors of long term response to AChE inhibitors in AD patients. *Journal of Neurology, Neurosurgery & Psychiatry*, *76*(8), 1064-1069. http://dx.doi.org/10.1136/jnnp.2004.051334

Di Lazzaro, V., Oliviero, A., Profice, P., Pennisi, M. A., Di Giovanni, S., Zito, G., Tonali, P., & Rothwell, J. C. (2000). Muscarinic receptor blockade has differential effects on the excitability of intracortical circuits in the human motor cortex. *Experimental Brain Research*, *135*(4), 455-461. https://doi.org/10.1007/s002210000543

Di Lazzaro, V., Oliviero, A., Saturno, E., Pilato, F., Insola, A., Mazzone, P., Profice, P., Tonali, P., & Rothwell, J. (2001). The effect on corticospinal volleys of reversing the direction of current induced in the motor cortex by transcranial magnetic stimulation. *Experimental Brain Research*, *138*(2), 268-273. https://doi.org/10.1007/s002210100722

Di Lazzaro, V., Profice, P., Ranieri, F., Capone, F., Dileone, M., Oliviero, A., & Pilato, F. (2012). I-wave origin and modulation. *Brain stimulation*, *5*(4), 512-525.

Dubbioso, R., Raffin, E., Karabanov, A., Thielscher, A., & Siebner, H. R. (2017). Centre-surround organization of fast sensorimotor integration in human motor hand area. *Neuroimage*, *158*, 37-47. https://doi.org/10.1016/j.neuoimage.2017.06.063

Dushanova, J., & Christov, M. (2014). The effect of aging on EEG brain oscillations related to sensory and sensorimotor functions. *Advances in medical sciences*, *59*(1), 61-67.

Economo, M. N., Viswanathan, S., Tasic, B., Bas, E., Winnubst, J., Menon, V., ... & Svoboda, K. (2018). Distinct descending motor cortex pathways and their roles in movement. *Nature*, *563*(7729), 79-84.

Edwards, L. L., King, E. M., Buetefisch, C. M., & Borich, M. R. (2019). Putting the "sensory" into sensorimotor control: the role of sensorimotor integration in goal-directed hand movements after stroke. *Frontiers in integrative neuroscience*, *13*, 16.

Engel, A. K., & Fries, P. (2010). Beta-band oscillations—signalling the status quo?. *Current opinion in neurobiology*, *20*(2), 156-165.

Fischer, P., Tan, H., Pogosyan, A., & Brown, P. (2016). High post-movement parietal low-beta power during rhythmic tapping facilitates performance in a stop task. *European Journal of Neuroscience*, *44*(5), 2202-2213.

Hallett, M. (2007). Transcranial magnetic stimulation: A primer. *Neuron*, *55*(2), 187-199. https://doi.org/10.1016/jneuron.2007.06.026

Hamada, M., Galea, J. M., Di Lazzaro, V., Mazzone, P., Ziemann, U., & Rothwell, J. C. (2014). Two distinct interneuron circuits in human motor cortex are linked to different subsets of physiological and behavioral plasticity. *Journal of Neuroscience*, *34*(38), 12837-12849.

Hannah, R., & Rothwell, J. C. (2017). Pulse duration as well as current direction determines the specificity of transcranial magnetic stimulation of motor cortex during contraction. *Brain Stimulation*, *10*(1), 106-115. https://doi.org/10.1016/j.brs.2016.09.008

Heinrichs-Graham, E., Wilson, T. W., Santamaria, P. M., Heithoff, S. K., Torres-Russotto, D., Hutter-Saunders, J. A., ... & Gendelman, H. E. (2014). Neuromagnetic evidence of abnormal movement-related beta desynchronization in Parkinson's disease. *Cerebral cortex*, *24*(10), 2669-2678.

Jensen, O., Gelfand, J., Kounios, J., & Lisman, J. E. (2002). Oscillations in the alpha band (9–12 Hz) increase with memory load during retention in a short-term memory task. *Cerebral cortex*, *12*(8), 877-882.

Kaňovský, P., Bareš, M., & Rektor, I. (2003). The selective gating of the N30 cortical component of the somatosensory evoked potentials of median nerve is different in the mesial and dorsolateral frontal cortex: evidence from intracerebral recordings. *Clinical neurophysiology*, *114*(6), 981-991.

Karakaş, S., Erzengin, Ö. U., & Başar, E. (2000). A new strategy involving multiple cognitive paradigms demonstrates that ERP components are determined by the superposition of oscillatory responses. *Clinical Neurophysiology*, *111*(10), 1719-1732.

Kelly, R. M., & Strick, P. L. (2003). Cerebellar loops with motor cortex and prefrontal cortex of a nonhuman primate. *Journal of neuroscience*, *23*(23), 8432-8444.

Kennerley, S. W., Sakai, K., & Rushworth, M. F. S. (2004). Organization of action sequences and the role of the pre-SMA. *Journal of neurophysiology*, *91*(2), 978-993.

Klimesch, W. (1996). Memory processes, brain oscillations and EEG synchronization. *International Journal of Psychophysiology*, *24*(1-2), 61-100. https://doi.org/10.1016/S0167-8760(96)00057-8

Klimesch, W., Doppelmayr, M., Pachinger, T., & Russegger, H. (1997). Event-related desynchronization in the alpha band and the processing of semantic information. *Cognitive Brain Research, 6*(2), 83-94. https://doi.org/10.1016/S0926-6410(97)00018-9

Klimesch, W., Doppelmayr, M., Schwaiger, J., Auinger, P., & Winkler, T. H. (1999). Paradoxical'alpha synchronization in a memory task. *Cognitive Brain Research*, *7*(4), 493-501.

Knyazev, G. G. (2012). EEG delta oscillations as a correlate of basic homeostatic and motivational processes. *Neuroscience & Biobehavioral Reviews*, *36*(1), 677-695.

Lansbergen, M. M., Arns, M., van Dongen-Boomsma, M., Spronk, D., & Buitelaar, J. K. (2011). The increase in theta/beta ratio on resting-state EEG in boys with attention-

deficit/hyperactivity disorder is mediated by slow alpha peak frequency. *Progress in Neuro-Psychopharmacology and Biological Psychiatry, 35*(1), 47-52. https://doi.org/10.1016/j.pnpbp.2010.08.004

Lara, A. H., Cunningham, J. P., & Churchland, M. M. (2018). Different population dynamics in the supplementary motor area and motor cortex during reaching. *Nature communications*, *9*(1), 1-16.

Lavie, N., Hirst, Aleksandra; de Fockert, Jan W.; Viding, Essi (2004). *Load Theory of Selective Attention and Cognitive Control. Journal of Experimental Psychology: General, 133(3), 339–354.* doi:10.1037/0096-3445.133.3.339

Lazzaro, I., Gordon, E., Li, W., Lim, C. L., Plahn, M., Whitmont, S., ... & Meares, R. (1999). Simultaneous EEG and EDA measures in adolescent attention deficit hyperactivity disorder. *International journal of psychophysiology*, *34*(2), 123-134.

Lehmann, S. J., & Scherberger, H. (2013). Reach and gaze representations in macaque parietal and premotor grasp areas. *Journal of Neuroscience*, *33*(16), 7038-7049.

Li, X., Honda, S., Nakajima, S., Wada, M., Yoshida, K., Daskalakis, Z. J., ... & Noda, Y. (2021). TMS-EEG research to elucidate the pathophysiological neural bases in patients with schizophrenia: a systematic review. *Journal of Personalized Medicine*, *11*(5), 388.

Loo, S. K., & Barkley, R. A. (2005). Clinical utility of EEG in attention deficit hyperactivity disorder. *Applied Neuropsychology*, *12*(2), 64-76. https://doi.org/10.1207/s15324826an1202_2

Machado, S., Cunha, M., Velasques, B., Minc, D., Teixeira, S., Domingues, C. A., ... & Ribeiro, P. (2010). Sensorimotor integration: basic concepts, abnormalities related to movement disorders and sensorimotor training-induced cortical reorganization. *Rev Neurol*, *51*(7), 427-436.

Mauguiere, F. (2005). Somatosensory evoked potentials: Normal responses, abnormal waveforms, and clinical applications in neurological disease. *Electroencephalography. Basic Principles, Clinical Applications, and Related Fields*, 1067-1119.

Minc, D., Machado, S., Bastos, V. H., Machado, D., Cunha, M., Cagy, M., ... & Ribeiro, P. (2010). Gamma band oscillations under influence of bromazepam during a sensorimotor integration task: an EEG coherence study. *Neuroscience letters*, *469*(1), 145-149.

Mirdamadi, J. L., Suzuki, L. Y., & Meehan, S. K. (2017). Attention modulates specific motor cortical circuits recruited by transcranial magnetic stimulation. *Neuroscience*, *359*, 151-158. https://doi.org/10.1016/j.neuroscience.2017.07.028

Ni, Z., Charab, S., Gunraj, C., Nelson, A. J., Udupa, K., Yeh, I. J., & Chen, R. (2011). Transcranial magnetic stimulation in different current directions activates separate cortical circuits. *Journal of Neurophysiology*, *105*(2), 749-756. https://doi.org/10.1152/jn.00640.2010

Omlor, W., Patino, L., Hepp-Reymond, M. C., & Kristeva, R. (2007). Gamma-range corticomuscular coherence during dynamic force output. *Neuroimage*, *34*(3), 1191-1198.

Pandya, D. N., Hallett, M., & Mukherjee, S. K. (1969). Intra-and interhemispheric connections of the neocortical auditory system in the rhesus monkey. *Brain research*, *14*(1), 49-65.

Pesaran, B., Nelson, M. J., & Andersen, R. A. (2008). Free choice activates a decision circuit between frontal and parietal cortex. *Nature*, *453*(7193), 406-409.

Pfurtscheller, G., & Da Silva, F. L. (1999). Event-related EEG/MEG synchronization and desynchronization: basic principles. *Clinical neurophysiology*, *110*(11), 1842-1857.

Pfurtscheller, G., & Klimesch, W. (1992). Event-related synchronization and desynchronization of alpha and beta waves in a cognitive task. In E. Basar & T. H. Bullock (Eds), *Induced Rhythms in the Brain*,117-128. Birkhäuser, Boston, MA. https://doi.org/10.1007/978-1-4757-1281-0_6

Pfurtscheller, G., Neuper, C., Andrew, C., & Edlinger, G. (1997). Foot and hand area mu rhythms. *International Journal of Psychophysiology*, *26*(1-3), 121-135.

Pfurtscheller, G., Stancak Jr, A., & Neuper, C. (1996). Event-related synchronization (ERS) in the alpha band—an electrophysiological correlate of cortical idling: A review. *International Journal of Psychophysiology*, *24*(1-2), 39-46. https://doi.org/10.1016/S0167-8760(96)00066-9

Puzzo, I., Cooper, N. R., Cantarella, S., & Russo, R. (2011). Measuring the effects of manipulating stimulus presentation time on sensorimotor alpha and low beta reactivity during hand movement observation. *NeuroImage*, *57*(4), 1358-1363.

Puzzo, I., Cooper, N. R., Cantarella, S., Fitzgerald, P. B., & Russo, R. (2013). The effect of rTMS over the inferior parietal lobule on EEG sensorimotor reactivity differs according to self-reported traits of autism in typically developing individuals. *Brain research*, *1541*, 33-41.

Rathelot, J. A., & Strick, P. L. (2009). Subdivisions of primary motor cortex based on cortico-motoneuronal cells. *Proceedings of the National Academy of Sciences*, *106*(3), 918-923.

Rothkegel, H., Sommer, M., Paulus, W., & Lang, N. (2010). Impact of pulse duration in single pulse TMS. *Clinical Neurophysiology*, *121*(11), 1915-1921. https://doi.org/10.1016/j.clinph.2010.04.006

Rothwell, J. C., Thompson, P. D., Day, B. L., Boyd, S., & Marsden, C. D. (1991). Stimulation of the human motor cortex through the scalp. *Experimental Physiology: Translation and Integration*, *76*(2), 159-200. https://doi.org/10.1113/expphysiol.1991.sp003485

Schmidt, R., Ruiz, M. H., Kilavik, B. E., Lundqvist, M., Starr, P. A., & Aron, A. R. (2019). Beta oscillations in working memory, executive control of movement and thought, and sensorimotor function. *Journal of Neuroscience*, *39*(42), 8231-8238.

Shin, J. (2011). The interrelationship between movement and cognition: Theta rhythm and the P300 event-related potential. *Hippocampus*, *21*(7), 744-752.

Simon, S. S., Tusch, E. S., Holcomb, P. J., & Daffner, K. R. (2016). Increasing working memory load reduces processing of cross-modal task-irrelevant stimuli even after controlling for task difficulty and executive capacity. *Frontiers in Human Neuroscience*, *10*, 380. https://doi.org/10.3389/fnhum.2016.00380

Spampinato, D. A., Celnik, P. A., & Rothwell, J. C. (2020). Cerebellar–motor cortex connectivity: one or two different networks?. *Journal of Neuroscience*, *40*(21), 4230-4239.

Stančák Jr, A., Feige, B., Lücking, C. H., & Kristeva-Feige, R. (2000). Oscillatory cortical

activity and movement-related potentials in proximal and distal movements. *Clinical

Neurophysiology*, *111*(4), 636-650. https://doi.org/10.1016/S1388-2457(99)00310-7

Stefan, K., Wycislo, M., & Classen, J. (2004). Modulation of associative human motor cortical

plasticity by attention. *Journal of neurophysiology*, *92*(1), 66-72.

Suzuki, L. Y., & Meehan, S. K. (2018). Verbal working memory modulates afferent circuits in

motor cortex. *European Journal of Neuroscience*, *48*(10), 3117-3125.

https://doi.org/10.1111/ejn.14154

Teplan, M. (2002). Fundamentals of EEG measurement. *Measurement science review*, *2*(2), 1-

11.

Thompson, T., Steffert, T., Ros, T., Leach, J., & Gruzelier, J. (2008). EEG applications for sport

and performance. *Methods*, *45*, 279-288.

Tokimura, H., Di Lazzaro, V., Tokimura, Y., Oliviero, A., Profice, P., Insola, A., Mazzone, P.,

Tonali, P., & Rothwell, J. C. (2000). Short latency inhibition of human hand motor cortex

by somatosensory input from the hand. *The Journal of Physiology*, *523*(Pt 2), 503-513.

https://doi.org/10.1111/j.1469-7793.20000.t01-1-00503.x

Tranchina, D., & Nicholson, C. (1986). A model for the polarization of neurons by extrinsically

applied electric fields. *Journal of Biophysiology, 50*(6), 1139-56. Doi: 10.1016/S0006-

3495(86)83558-5

Turco, C. V., El-Sayes, J., Locke, M. B., Chen, R., Baker, S., & Nelson, A. J. (2018a). Effects of lorazepam and baclofen on short-and long-latency afferent inhibition. *The Journal of Physiology*, *596*(21), 5267-5280. https://doi.org/10.1113/JP276710

Turco, C. V., El-Sayes, J., Savoie, M. J., Fassett, H. J., Locke, M. B., & Nelson, A. J. (2018b). Short-and long-latency afferent inhibition; uses, mechanisms and influencing factors. *Brain Stimulation*, *11*(1), 59-74. https://doi.org/10.1016/j.brs.2017.09.009

Wise, S. P., & Kurata, K. (1989). Set-related activity in the premotor cortex of rhesus monkeys: effect of triggering cues and relatively long delay intervals. *Somatosensory & motor research*, *6*(5-6), 455-476.

Zhang, Z. W., & Descheˆnes, M. (1997). Intracortical axonal projections of lamina VI cells of the primary somatosensory cortex in the rat: a single-cell labeling study. *Journal of Neuroscience*, *17*(16), 6365-6379.

Ziemann, U., Reis, J., Schwenkreis, P., Rosanova, M., Strafella, A., Badawy, R., & Müller-Dahlhaus, F. (2015). TMS and drugs revisited 2014. *Clinical Neurophysiology*, *126*(10), 1847-1868. https://doi.org/10.1016/j.clinph.2014.08.028